

Quantitative Analysis of Amino Acid Oxidation and Related Gluconeogenesis in Humans

ROBERT L. JUNGAS, MITCHELL L. HALPERIN, AND JOHN T. BROSNAN

*Department of Physiology, University of Connecticut Health Center, Farmington, Connecticut;
Department of Medicine, St. Michael's Hospital, University of Toronto, Toronto, Ontario;
and Department of Biochemistry, Memorial University, St. John's, Newfoundland, Canada*

I. Introduction	419
II. Problem to be Analyzed	420
III. Events in Small Intestine	420
A. Acid-base balance	421
B. Energy balance	423
IV. Events in Muscle	423
A. Acid-base and energy balances	427
V. Events in Kidney	427
A. Acid-base and energy balances	428
VI. Events in Liver	428
A. Assumptions	430
B. Pathway of carbon and nitrogen flow	431
C. Acid-base and energy balances	433
D. Observations	435
VII. Whole Body Energy Balance	436
VIII. Metabolic Processes	436
IX. Liver Oxidation of Amino Acids	438
X. Intestinal Oxidation of Amino Acids	439
XI. Cholesterologenesis	439
XII. Metabolic Pathways in Liver	440
XIII. Role of Urease	441
XIV. Compartmenting of Urea Cycle	441
XV. Mitochondrial Acid-Base Balance	442
XVI. Whole Body Acid-Base Balance	443
XVII. Summary	443

I. INTRODUCTION

We present an overview of our present knowledge of amino acid catabolism in humans, utilizing the problem-solving approach currently popular in medical education. The result is not a systematic review but a synthesis of current knowledge aimed at providing as accurate a quantitative description of amino acid catabolism in humans as current data permit. Readers working through the synthesis will find that they have in fact reviewed much of what is known of amino acid catabolism in higher animals.

Important advances in our understanding of intermediary metabolism have resulted from the quantitative analysis of pathway fluxes. Unfortunately such analyses are usually complicated, even for relatively simple pathways. Our present attempt to analyze one of the most complex of metabolic processes, the complete catabolism of dietary amino acids as it occurs daily in humans, is no exception. Although our analysis is less

than optimal because of the unavailability of certain data, significant conclusions appear justifiable. We find hepatic gluconeogenesis from a natural mixture of amino acids to be nearly perfectly balanced energetically, i.e., those metabolic steps that produce ATP are precisely matched by steps that utilize ATP. The large ATP yield that would result prohibits the complete oxidation of amino acids to CO₂ in the liver, whereas the partial oxidation of amino acids as they are converted to glucose provides exactly the energy needed to support gluconeogenesis. Even this partial oxidation of the normal daily dietary supply of amino acids accounts for about one-half of the daily O₂ consumption of the liver, making amino acids the major fuel utilized by liver for ATP production. Gluconeogenesis from amino acids must, therefore, be regarded as a normal prandial process, not one limited to fasting periods.

From our analysis we conclude that the main pathway of carbon flow during gluconeogenesis from a balanced mixture of amino acids differs importantly from

that commonly presented in textbooks (16, 42, 48, 70). The overall process of amino acid oxidation in the liver is so designed that the potential alkalotic threat associated with amino acid oxidation pointed out by Atkinson and Bourke (4) is never realized. Instead amino acid oxidation invariably generates strong nonvolatile acid. This metabolic fixed-acid load is normally largely neutralized not by urinary acid excretion but by the metabolic generation of bicarbonate associated with the hepatic oxidation of dietary anions or the renal oxidation of glutamine (30).

We offer the view that "uncoupled" O_2 consumption via the mitochondrial respiratory chain proton pump occurs regularly during hepatic amino acid oxidation. Indeed such a process appears to be essential for the maintenance of acid-base balance within liver mitochondria.

II. PROBLEM TO BE ANALYZED

We seek a quantitative description of the energy and acid-base balances associated with the conversion of the mixture of amino acids present in a typical daily diet to CO_2 , water, sulfate, and nitrogenous end products. Our approach is to work through a specific example as precisely as current knowledge permits, seeking conclusions of general significance. To simplify the calculations the amino acids are considered to be metabolized entirely in just four organs: the small intestine, skeletal muscle, the kidneys, and the liver. Only major metabolic pathways are included.

It is obvious that to describe in quantitative terms so complex a metabolic process requires many assumptions. Indeed, some may argue that our knowledge base is still so limited that the entire effort is futile. We disagree. We can even at this time make an instructive initial effort in this direction, recognizing that our estimates will be in need of updating when new data become available.

For our purposes, the example to be analyzed must begin with exactly defined amino acid inputs. An active adult male in a steady state oxidizes ~100–125 g of protein daily (21, 35). We assume that the amino acid composition of this protein is typical of meats, such as beef, chicken, pork, or lamb, and that it contains 1,000 mmol amino acids and 1,400 mmol nitrogen distributed exactly as shown in Table 1 (27a, 47). The pH of this protein mixture is assumed to be 6.8 as is typical for muscle proteins after boiling, and the average acid dissociation constant of its histidine residues is also assumed to be 6.8 [an average for 21 determinations (20)].¹

¹ We estimate a dietary input of anions such as malate, lactate, and citrate of 50 mmol, but since their processing is conveniently considered separately from amino acids we use this input only in calculating net acid-base balance. For the latter purpose we also assume 40 mmol phosphorus (1,240 mg) are present in the daily diet, of which 30 mmol are absorbed and excreted. Of this 30 mmol, 16 mmol are considered equivalent to HPO_4^{2-} and 14 mmol are equivalent to $H_2PO_4^-$ (30) so that urinary titratable acidity cannot exceed 16 meq/day in the steady state.

TABLE 1. *Dietary amino acid input*

Amino Acid	mmol/day				
	N to urea or NH_4^+	C atoms	HCO_3^- formed	H atoms	O atoms
Alanine	78	78	234	78	546
Aspartate	38	38	152	76	228
Asparagine	62	124	248	124	496
Arginine	46	160	276	114	690
Cysteine	12	12	36	12	84
Glutamine	56	112	280	112	560
Glutamate	70	70	350	140	560
Glycine	98	86	196	86	490
Histidine	30	90	180	74*	286*
Lysine	76	152	456	76	1140
Leucine	84	84	504	84	1092
Isoleucine	56	56	336	56	728
Methionine	24	24	120	24	264
Phenylalanine	32	32	288	32	352
Proline	52	52	260	52	468
Serine	50	50	150	50	350
Threonine	48	48	192	48	432
Tryptophan	8	16	88	16	96
Tyrosine	26	26	234	26	286
Valine	54	54	270	54	594
Totals	1,000	1,364†	4,850	1,334‡	9,742

The total weight of protein that provides the amino acids shown is 110 g, which following hydrolysis will yield 128 g of amino acids.

* Only 16 of 30 histidines were assumed to be protonated on both ring N atoms. † Another 12 N atoms of glycine and 24 of arginine are converted to creatinine, giving a total of 1,400. ‡ Creatinine formation reduces HCO_3^- generation by 36 mmol/day. The load of fixed acid derived from nonsulfur amino acids equals $1,364 - 1,334$ or 30 and is unaltered by creatinine formation.

III. EVENTS IN SMALL INTESTINE

We begin by considering the major events that occur in the duodenum and jejunum of the small intestine, hereafter frequently referred to simply as the gut. Not all of the dietary amino acids absorbed from the gut lumen reach the portal vein, as shown by Windmueller and Spaeth (66, 67). Nearly all of the glutamate and aspartate and perhaps two-thirds of the dietary glutamine are metabolized within mucosal cells during their transport (68). Glutamine that is released mainly from muscle and provided to the gut via the mesenteric arteries is also an important fuel for this tissue. Figure 1 presents a simplified view of the metabolic process occurring in the gut during amino acid absorption, with a more realistic view shown in Figure 8 of APPENDIX B for readers who want to follow the details of the metabolic calculations to be introduced. The α -amino nitrogen of the three amino acids consumed in the gut appears in the portal vein mainly as alanine, whereas the amide nitrogen of glutamine is released by glutaminase and appears as NH_4^+ . The carbon of these amino acids is converted largely to CO_2 and lactate. Glucose is not a major oxidative fuel for the gut, and very little oxidation to CO_2 occurs, as it is absorbed from the lumen. Some glycolysis does occur, however, so that the major source of the carbon appearing as portal vein alanine is glucose.

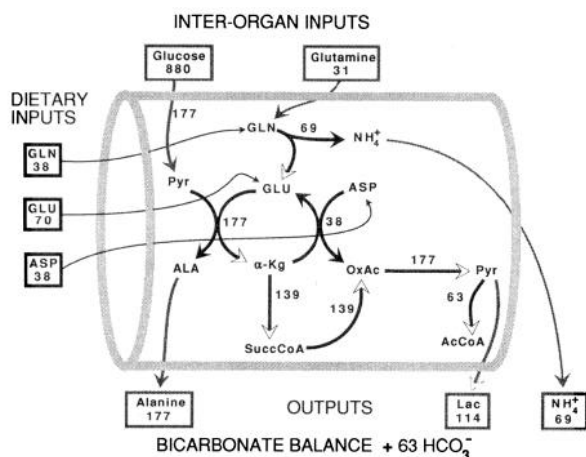


FIG. 1. Metabolic process occurring in small intestine during oxidation of daily supply of amino acids in humans. Three dietary amino acids consumed by gut are shown on *left* enclosed in boxes, with number in each box indicating millimoles oxidized per day. In addition, glucose and some glutamine released mainly from muscle are provided by mesenteric arteries, as shown at *top*. Blood glucose serves as major source of alanine carbon, which is shown exiting to portal vein at *bottom*. Other end products are lactate, NH₄⁺, and CO₂. Net amount of product formed in each step (in mmol/day) is indicated by number associated with each arrow. Pathway of flow of glutamine carbon to lactate and acetyl-CoA is shown by arrows with open arrowheads. AcCoA, acetyl-CoA; α-Kg, α-ketoglutarate; Lac, lactate; OxAc, oxaloacetate; Pyr, pyruvate; SuccCoA, succinyl-CoA. See Fig. 8 in APPENDIX B for more complete portrayal.

About one-third of dietary arginine is also metabolized during intestinal transport, with the nitrogen appearing as urea, ornithine, and citrulline (23, 67). The citrulline released into the portal vein is largely ignored by the liver and is instead taken up by the kidneys, which convert it back to arginine (69). This is an important process, as it allows a significant fraction, perhaps one-half, of dietary arginine to bypass the arginase of the liver and reach the peripheral tissues, but we omitted these events from our diagrams for simplicity.

One of our goals is to calculate the overall balance of ATP and of protons and bicarbonate, i.e., the acid-base balance, for the metabolic process occurring in the gut. These calculations are summarized in Table 2. The two major metabolic compartments of the mucosal cells are listed along with the reactions that occur in each. Only reactions that affect either the ATP balance or the acid-base balance are listed. For each reaction the number of protons and the amount of ATP directly produced or consumed are shown. If a reaction consumes protons, CO₂ is considered to be hydrated to H⁺ and HCO₃⁻ to provide the needed protons, and bicarbonate is viewed as a product of the step (note last reaction in Table 2). In addition the amount of reduced pyridine nucleotides or reduced flavoproteins generated is listed so that the ATP balance following the reoxidation of these substances via the respiratory chain can be calculated.

Any bicarbonate consumed by CO₂ fixation reactions is listed along with any CO₂ produced by decarboxylation reactions. These latter values are essential in computing the acid-base balance and for checking that

all carbon atoms have been accounted for. For our purposes, steps that consume or generate bicarbonate by consuming or generating CO₂ must be distinguished from those that consume or generate bicarbonate by generating or consuming protons. Only in the latter case does a net metabolic production or consumption of non-volatile acid occur that cannot be accommodated by the lungs (Fig. 2).

The accuracy of the acid-base calculations can be checked by keeping track of the net charge of all metabolite input to and output from each cellular compartment, as noted in Table 2. We know of no similar way to check the accuracy of the ATP calculations, but all O₂ uptake calculations were verified by noting the number of oxygen atoms present in all inputs and outputs, including water.

A. Acid-Base Balance

The results of these calculations indicate that although there is no net production of nonvolatile acid or base in the cytoplasm of the intestinal cells, there is a net consumption of protons in the mitochondrial compartment. If nothing else intervened, this proton deficiency would have to be met by the concurrent production of protons via mitochondrial carbonic anhydrase (24), as shown in *reaction 14* of Table 2. We thus arrive at the conclusion that there is a net production of ~63 mmol bicarbonate/day within the small intestinal mucosal cells as the daily load of dietary amino acids is processed.

Although this conclusion is valid for the intestinal cells as a whole, the data are incomplete. Because the metabolic reactions occur partly in the cytoplasm and partly in the mitochondrial matrix, there are substantial fluxes of metabolites across the inner mitochondrial membrane. It is essential to keep track of the energy expenditure and the proton movements associated with these transport events if we are to arrive at an accurate assessment of the balances in the separate cellular compartments. We summarize these transport steps in Table 3 along with the energetic and acid-base implications of each. Each recognized carrier involved is listed along with the number of protons and/or positive charges translocated with it. Our best estimate of the net effect of the operation of these carriers is the translocation of 196 mmol protons into the mitochondria, i.e., down the proton-motive force gradient established by the respiratory chain proton pump. Note, however, that the number of positive charges entering the mitochondrial matrix does not equal the number of protons, being only 133 mmol. Therefore it is necessary to calculate the energy costs of these translocations separately, and we did so in the manner suggested in Table 3. The net effect is an energy cost of ~37 mmol ATP/day, mostly as a result of the charge movements occurring.

We are now in a position to more accurately assess the effects of amino acid metabolism on the acid-base balance of the cellular compartments of the gut. In the

TABLE 2. Balance of ATP, CO₂, and HCO₃⁻ in gut

Reactions in Cytoplasm	mmol/day					
	H ⁺	CO ₂	HCO ₃ ⁻	ATP	NADH	FPH ₂
1 Glucose → 2 GAP	0	0	0	-177	0	0
2 GAP → 1,3-BPG ⁻ + H ⁺	177	0	0	0	177	0
3 1,3-BPG ⁻ → 3-PGA ⁻	0	0	0	177	0	0
4 OxAc ²⁻ + H ⁺ → PEP ⁻ + CO ₂	-177	177	0	-177	0	0
5 PEP ⁻ → Pyr ⁻	0	0	0	354	0	0
6 Pyr ⁻ → Lac ⁻	0	0	0	0	-114	0
7 OxAc ²⁻ → Mal ²⁻	0	0	0	0	-63	0
Totals	0	177	0	177	0	0

Reactions in Mitochondria	mmol/day					
	H ⁺	CO ₂	HCO ₃ ⁻	ATP	NADH	FPH ₂
8 Pyr ⁻ → AcCoA ⁻ + CO ₂	0	63	0	0	63	0
9 Isocit ³⁻ + H ⁺ → α-KG ²⁻ + CO ₂	-63	63	0	0	63	0
10 α-KG ²⁻ → SuccCoA ²⁻ + CO ₂	0	202	0	0	202	0
11 SuccCoA ²⁻ → Succ ²⁻	0	0	0	202	0	0
12 Succ ²⁻ → Fum ²⁻	0	0	0	0	0	202
13 Mal ²⁻ → OxAc ²⁻	0	0	0	0	265	0
Totals	-63	328	0	202	593	202
14 CO ₂ + H ₂ O → H ⁺ + HCO ₃ ⁻	63	-63	63			
Net balances	0	265	63			
Net HCO ₃ ⁻ balance of gut			63			

Equivalent O ₂ uptake	296 ^{1/2}	101
Total O ₂ uptake		
H _{out} ⁺ by respiratory chain*	7,116	1,616
Total H _{out} ⁺ by respiratory chain	8,732	

Consequences of metabolic reactions only are given; events associated with metabolite transport across membranes are not included. To simplify these reactions, ATP and its products, ADP and P_i, were omitted, and charges associated with phosphate groups were ignored. Similarly, redox coenzymes are shown only as tabular entries, ignoring their charge. Carboxyl groups esterified to CoA were treated as carboxylate anions. These conventions do not introduce errors, since phosphate groups and coenzymes function catalytically in steady state. Net charge of all metabolite input to gut cytoplasm (except bicarbonate and phosphates) is -366, whereas that of all products released is -366, so there can be no net change in charge resulting from metabolic reactions. Corresponding values for gut mitochondria are -322 and -259, so metabolic reactions in that compartment must lead to an increase in charge of 63. These numbers provide a convenient check on the proton plus bicarbonate balance. FPH₂, reduced flavoproteins; GAP, glyceraldehyde 3-phosphate; 1,3-BPG, 1,3-bisphosphoglycerate; 3-PGA, 3-phosphoglycerate; OxAc, oxoacetic acid; PEP, phosphoenolpyruvate; Pyr, pyruvate; Lac, lactate; Mal, malate; AcCoA, acetyl-CoA; Isocit, isocitrate; α-KG, α-ketoglutarate; SuccCoA, succinyl-CoA; Succ, succinate; Fum, fumarate. * Based on 12 protons per NADH and 8 per FPH₂.

mitochondrial matrix, although the chemical reactions generate a net production of 63 mmol bicarbonate, the 196 mmol protons entering the matrix via the metabolite carriers reverse the balance so that a net bicarbonate deficit will develop at the rate of 133 mmol/day. In a steady state this cannot continue. Some means must be found to translocate protons or bicarbonate between the

cytoplasmic and mitochondrial compartments. In the absence of any clear evidence for the existence in the inner mitochondrial membrane of a specific bicarbonate carrier system, the only process of sufficient magnitude that appears to be available for this purpose is the movement of protons via the respiratory chain. Accordingly, we conclude that 133 of the 8,732 mmol protons that are pumped out of the mitochondrial matrix by the respiratory chain (Table 2) must react with bicarbonate in the cytoplasm rather than recycling back to the matrix via the ATP-synthetase.

We thus assign an additional function to the respiratory chain proton pump, that of maintaining acid-base balance in the mitochondrial matrix. Note that the energetic cost of maintaining the matrix proton balance is very small; only 1.5% of the protons pumped out of the matrix by the respiratory chain during amino acid oxidation need be diverted. Because this small quantity of protons does not recycle into the matrix through the ATP-synthetase, the electron flow to O₂ required for

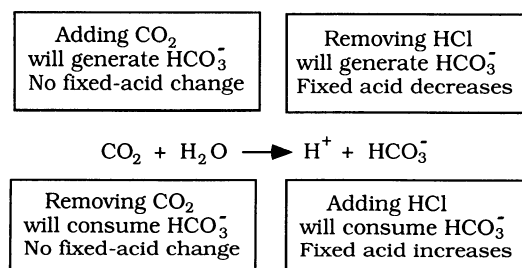


FIG. 2. Relation of changes in bicarbonate to changes in fixed (nonvolatile) acid.

TABLE 3. Proton and charge movements associated with mitochondrial metabolite transport in gut

Translocation Process	Type	mmol/day			
		Protons		Positive charge	
		In	Out	In	Out
1 Asp ⁻ _{out} /Glu ⁻ _{in} · H ⁺ _{in}	Antipport	202		202	
2 Glu ⁻ _{out} /H ⁺ _{out}	Symport		69		
3 Pyr ⁻ _{in} /H ⁺ _{in}	Symport	63			
4 Gln _{in} (69)	Neutral entry				
5 NH ⁺ ₄ _{out}	*				69
6 α-KG ²⁻ _{out} /Mal ²⁻ _{in} (63)	Antipport				
Totals		265	69	202	69
Net		196		133	

$$\text{ATP cost of translocation} = 196 \times 1/16 + 133 \times 3/16 \\ = 12\frac{1}{4} + 24\frac{15}{16} \approx 37$$

Movements of protons or positive charge into or out of mitochondria. Numbers in parentheses are millimoles per day of substances transported without obligatory proton or charge movements. For the purpose of estimating energy costs of metabolite transport, it was assumed that 4 protons enter mitochondrion during synthesis of 1 ATP and that $\frac{1}{4}$ of proton-motive force ($\Delta p = 60\Delta pH + \Delta\Psi$) across the inner mitochondrial membrane arises from ΔpH term and $\frac{3}{4}$ from $\Delta\Psi$ term (electrical potential difference across inner mitochondrial membrane in mV). Thus movement of a proton into a mitochondrion by an electroneutral process has a cost equivalent to $\frac{1}{4} \times \frac{1}{4} = \frac{1}{16}$ of a cytoplasmic ATP, whereas movement of a single positive charge into a mitochondrion has a cost equivalent to $\frac{3}{4} \times \frac{1}{4} = \frac{3}{16}$ of an ATP. For definitions of abbreviations see Table 2. * Translocation of positive charge associated with NH₄⁺ exit is not intended to imply any specific mechanism. Whether NH₄⁺ exits as a cation on an antiport or symport or exits as NH₃ with H⁺ exiting separately, the overall effect will be as shown in the steady state, unless protons other than those present in the NH₄⁺ cation are involved.

pumping these protons out of the matrix constitutes a form of "uncoupled respiration." Carefully regulated uncoupled respiration may serve, therefore, as a means of generating needed warmth, of dissipating excess calories, or of maintaining matrix pH balance.

A summary of the bicarbonate balances involved as amino acids are processed in the gut is given in Figure 3, *top left*. The remainder of Figure 3 shows the relationship between these events in the gut and whole body acid-base balance. Each is discussed in turn as we proceed with our analysis.

B. Energy Balance

Turning to the ATP balance in the small intestine, we note from Table 2 that there is a net production of ATP at the substrate level in both cytoplasm and matrix. Reoxidation of the reduced coenzymes produced will lead to a net O₂ consumption of ~400 mmol/day. This is accompanied by the translocation via the respiratory chain of nearly 9 mol protons from the matrix into the cytoplasm, assuming that the 12-proton model of Lemasters (43) is correct. Before calculating the amount of ATP that can be generated via the mitochondrial inner membrane ATP-synthetase as these protons reenter

the matrix, we must adjust this number according to the needs of acid-base balance as indicated and consider one other complicating factor.

This complication arises from the fact that ATP, which is synthesized by oxidative phosphorylation and utilized within the mitochondrial matrix, never has to be transported into the cytoplasm as does the bulk of newly made ATP. Because transporting one P_i and one ADP into a mitochondrion and one ATP out results in the movement of one proton into the mitochondrial matrix (41), this means that only three protons must reenter the matrix for each ATP made and utilized within the matrix, whereas four protons must enter for each ATP synthesized and exported to the cytoplasm. Thus to calculate how many millimoles of ATP can be synthesized from a given number of protons, one must know in what compartment the ATP will be utilized. Unfortunately, there are no rigorous data available to help us. We are forced to make an assumption and have decided to allocate to the cytoplasm 90% of the excess ATP made available from the process of amino acid oxidation. On this basis we calculate a positive net ATP balance in the small intestine of 2,328 mmol/day, as shown in Table 4. This number includes an allowance of 184 mmol ATP required for the active uptake of amino acids and di- and tripeptides from the gut lumen during protein digestion.

IV. EVENTS IN MUSCLE

Next we consider the metabolic process that occurs in skeletal muscle as the daily supply of amino acids is oxidized. Figure 4 presents a greatly simplified view of this process, with a more realistic view shown in Figure 9 of APPENDIX B for readers wanting to follow the details of the metabolic calculations. It is well established that in humans the bulk of the metabolism of the branched-chain amino acids (BCAA) begins in muscle. We recognize that BCAA are metabolized to a lesser extent in many other organs, but for our purposes it suffices to lump these organs together with muscle. Recent data indicate that the liver does process significant quantities of leucine, mainly by a mitochondrial pathway (50). Accordingly, we assume in Figure 4 that only 64 of the 84 mmol leucine supplied by the diet are utilized in muscle, along with all 56 mmol dietary isoleucine and 54 mmol valine.

Our understanding of the process occurring in muscle has been greatly advanced by the studies reported by Elia and Livesey (19). Muscle normally releases large quantities of alanine in the basal postprandial state, and this release is increased during fasting (22, 52). Much of this alanine is taken up by the liver and converted to blood glucose, which in turn serves as a major source of the alanine carbon released by muscle (11). This so-called "alanine cycle" (22, 46) serves to transport nitrogen derived from the breakdown of muscle protein to the liver for conversion to urea. Elia and Livesey (19) showed clearly, however, that the nitrogen

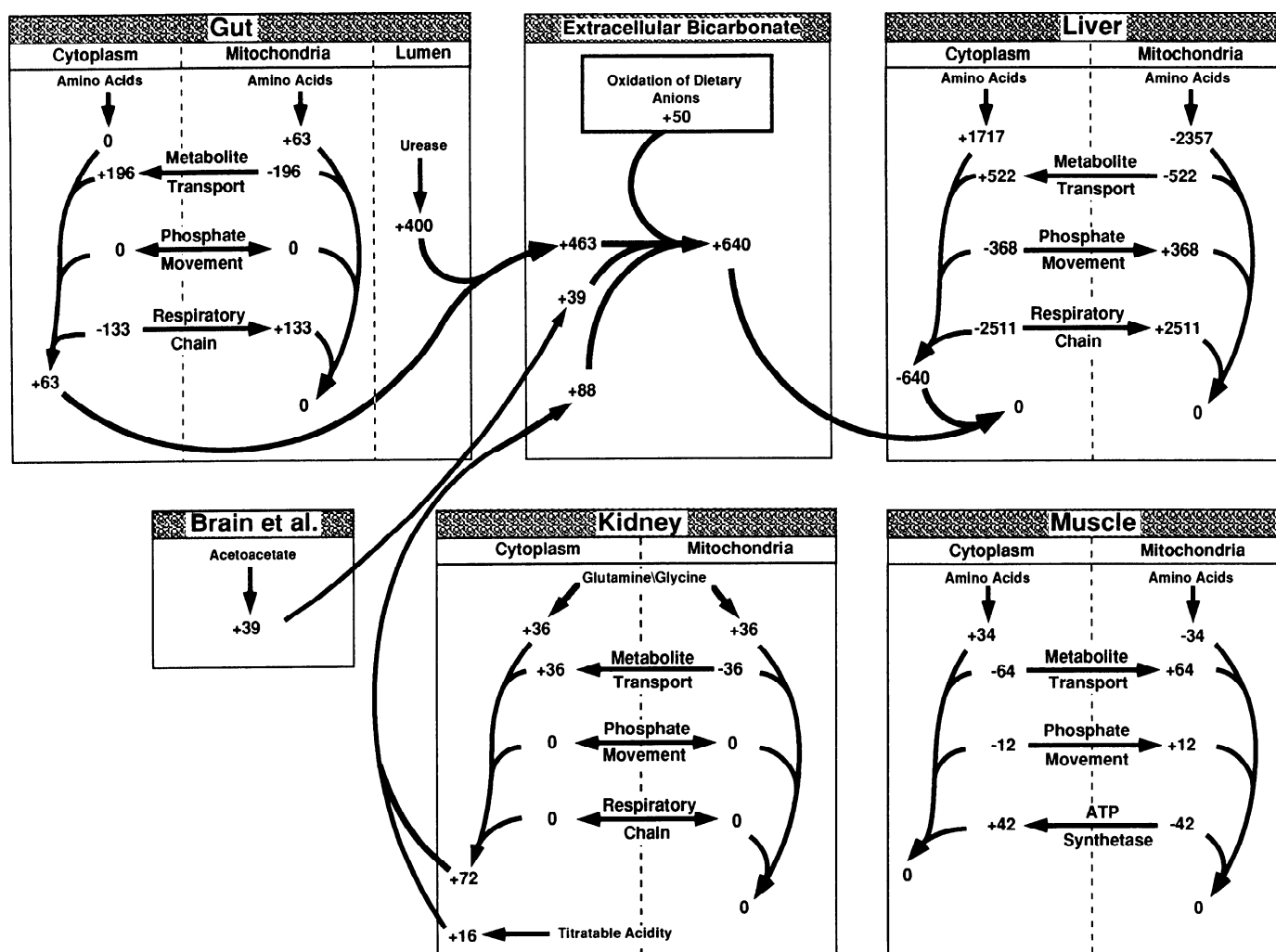


FIG. 3. Bicarbonate balances of several organs involved in oxidation of daily supply of amino acids in humans. Numbers indicate bicarbonate production (+) or consumption (−) (in mmol/day). Organs on left contribute bicarbonate to extracellular pool; liver consumes this bicarbonate and more, leaving a net deficit of 50 mmol/day, which is shown here as supplied by oxidation of dietary anions. Movement of protons across inner mitochondrial membrane either with metabolites or via respiratory chain is shown in bicarbonate equivalents.

derived from the BCAA contained in a protein meal or a leucine infusion was released from muscle largely as glutamine. In fact the consumption of glucose and the release of alanine were reduced under these conditions compared with their basal values. Apparently when BCAA become abundantly available for oxidation in muscle, both glucose oxidation and glycolysis to pyruvate are reduced by mechanisms similar to those brought into play when fatty acids or ketone bodies are provided to muscle. Accordingly, we have not shown a functioning alanine cycle in Figure 4. Instead we show ~90% of the nitrogen derived from the BCAA being released as glutamine and only ~10% released as alanine, consistent with the data of Elia and Livesey (19).

Figure 4 traces the flow of carbon from the BCAA to either glutamine or alanine. Initially acetyl-CoA is generated from leucine and isoleucine, whereas propionyl-CoA is formed from valine and isoleucine. Most of the acetyl-CoA simply enters the tricarboxylic acid cycle and is oxidized to CO₂. The propionyl-CoA is car-

boxylated to form oxaloacetate, most of which condenses with acetyl-CoA forming citrate. This citrate is then converted to glutamine and secreted. The amount of oxaloacetate generated is greater than needed to form the glutamine that is released. This excess oxaloacetate flows to pyruvate and is utilized to form the alanine that is released under these conditions. One is left with an excess of pyruvate that is shown as oxidized to CO₂ via the tricarboxylic acid cycle rather than as reduced to lactate, since there is no obvious source of cytoplasmic NADH and lactate production is diminished by the BCAA (19).

It is clear from Figure 4 that some of the potential gluconeogenic precursor, propionyl-CoA, is directly oxidized to CO₂ rather than being secreted as alanine to be later converted to glucose by liver. Of the propionyl-CoA converted to glutamine, secreted by muscle, and taken up by the gut, we have seen that one-third is oxidized to CO₂. The remainder of the glutamine secreted by muscle is metabolized in the kidneys where 20% is oxidized to

TABLE 4. Calculation of the ATP balance of the gut

	mmol/day		
Total H ⁺ _{out} by respiratory chain (Table 2)	8,732		
H ⁺ _{out} by uncoupled respiration (Fig. 3)	-133		
Total H ⁺ _{out} available for oxidative phosphorylation	8,599		
Net mitochondrial ATP from amino acids*		235	235
Mitochondrial ATP made at substrate level (Table 2)		202	
Mitochondrial ATP made by oxidative phosphorylation		33	
H ⁺ _{in} used to make mitochondrial ATP (×3)	99		
Remaining H ⁺ _{in} balance	8,500		
Cytoplasmic ATP by oxidative phosphorylation (÷4)		2,125	
Cytoplasmic ATP at substrate level (Table 2)		177	
Cytoplasmic ATP used to transport positive charge (Table 3)†		-25	
Cytoplasmic ATP used for amino acid transport‡		-184	
Net cytoplasmic ATP from amino acids		2,093	2,093
Net ATP balance of gut			2,328

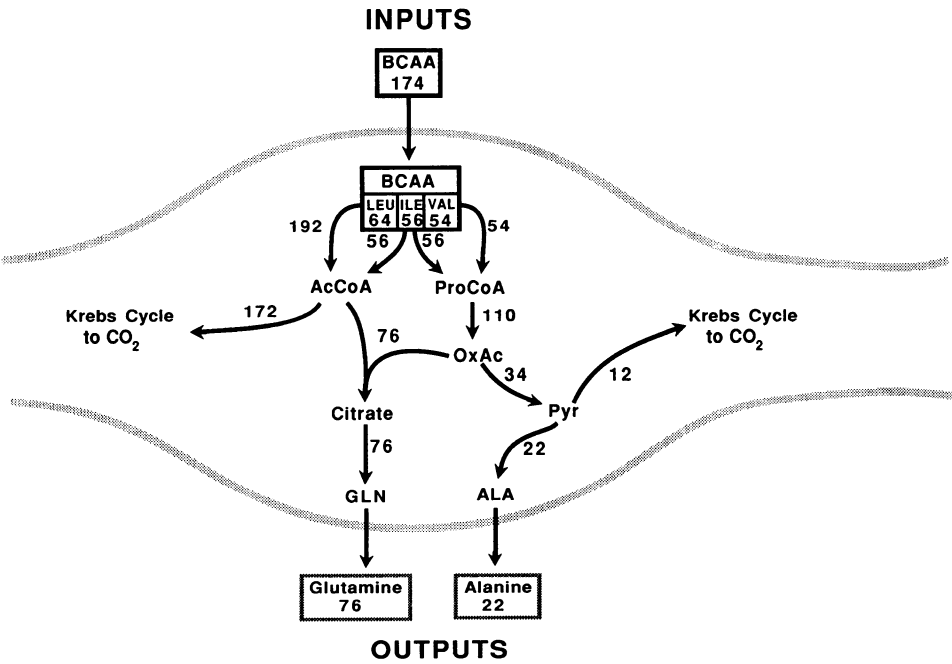
The 12-proton model of Lemasters (43) has been used as the basis of all ATP calculations. It was assumed that 4 protons with their net charges enter a mitochondrion through proton-translocating ATPase and adenylate and phosphate carriers during the synthesis of 1 cytoplasmic ATP so that P/O ratio is 3.0 for NADH and 2.0 for succinate. * It was assumed that the consumption of ATP by reactions external to the amino acid oxidation process was 90% cytoplasmic and 10% mitochondrial. That is, of 2,328 mmol ATP shown to be made available to the gut each day as a result of amino acid oxidation, 235 mmol were assumed to be utilized in the mitochondrial matrix. The 235 mmol are not exactly 10% of the total because we wanted to change the mitochondrial utilization of ATP in steps of 4 so that the ATP yield in each compartment would be an integer. † Only the ATP cost of transporting positive charge is included because the movement of protons has already been included in the adjustment for uncoupled respiration. ‡ Cost of amino acid transport was calculated on the assumption that all amino acids except glutamate and aspartate are actively transported into mucosal cells via a symport mechanism along with 1 Na⁺ and leave the cells via passive facilitated diffusion. Each Na⁺ was considered equivalent to 1/3 of a cytoplasmic ATP or ~4,000 cal/mol. Because the electrical potential across the jejunal mucosa luminal membrane is ~40 mV, 1/4 of energetic cost of pumping Na⁺ was attributed to electrical term and 3/4 to concentration gradient term. Thus when net cationic amino acid entry exceeds net anionic entry as it does in the gut, each extra positive charge entering the cell was considered to cost 1/12 ATP. One-third of amino acids were taken up as free amino acids, 1/3 as dipeptides, and 1/3 as tripeptides. Dipeptides and tripeptides were assumed to enter mucosal cells along with a single H⁺, considered energetically equivalent to Na⁺.

CO₂. Overall, 32 of the 110 mmol propionyl-CoA generated, or ~30%, will go to CO₂, whereas 70% goes to glucose via alanine (muscle), lactate (gut), or serine (kidneys). In long-term fasting or diabetes an even larger fraction of the propionyl-CoA is converted to glucose, since the major nitrogenous product secreted by muscle would then be alanine, not glutamine, and much

of the glutamine secreted would be converted by the kidneys to glucose. Thus in humans, valine and isoleucine serve as effective gluconeogenic amino acids even though their metabolism is initiated in an organ unable to secrete glucose.

Elia and Livesey (19) also measured the release of branched-chain α-keto acids (BCKA) from human mus-

FIG. 4. Metabolic process occurring in muscle during oxidation of daily supply of amino acids in humans. Only inputs are 3 branched-chain amino acids (BCAA) enclosed in box, which together amount to 174 mmol/day. Net amount of product formed in each step (in mmol/day) is indicated by number associated with each arrow. See Fig. 9 in APPENDIX B for more complete portrayal. ProCoA, propionyl-CoA. For definitions of other abbreviations see Fig. 1.



cle after a protein meal and found it to be only 3% of the amount of BCAA consumed by the muscle. For simplicity we show the entirety of the BCAA as metabolized by muscle. This clearly differs from the situation in other dietary conditions and in other species (33, 64). We also ignore the possibility that significant quantities of 3-OH-isobutyrate formed from valine may be released from muscle to be converted to glucose by the liver or kidney, a process likely to be of considerable significance in rats (44).

We set the amount of ammonium derived from amino acid metabolism and released into the blood to

zero, although a small amount may be released. This means that the rate of ammonium formation via glutamate dehydrogenase (76 mmol/day) was set equal to the rate of glutamine synthesis. It should be stressed that although glutamate dehydrogenase has relatively low activity in skeletal muscle, recent assays of human muscle performed in the presence of the activator, ADP, reveal the presence of 100 times the amount of this enzyme needed to process the daily dietary loads of BCAA (25, 54). We, therefore, have not utilized the Lowenstein purine cycle to generate the NH_4^+ needed for glutamine synthesis in resting muscle.

TABLE 5. Balance of ATP, CO_2 , and HCO_3^- in muscle

Reactions in Cytoplasm	mmol/day					
	H^+	CO_2	HCO_3^-	ATP	NADH	FPH ₂
1 $\text{OxAc}^{2-} + \text{H}^+ \rightarrow \text{PEP}^- + \text{CO}_2$	-34	34	0	-34	0	0
2 $\text{PEP}^- \rightarrow \text{Pyr}^-$	0	0	0	34	0	0
3 $\text{Glu}^- + \text{NH}_4^+ \rightarrow \text{Gln}$	0	0	0	-76	0	0
Totals	-34	34	0	-76	0	0
4 $\text{CO}_2 + \text{H}_2\text{O} \rightarrow \text{H}^+ + \text{HCO}_3^-$	34	-34	34	0	0	0
Net balances	0	0	34	-76	0	0

Reactions in mitochondria	mmol/day					
	H^+	CO_2	HCO_3^-	ATP	NADH	FPH ₂
5 $\text{Pyr}^- \rightarrow \text{AcCoA}^- + \text{CO}_2$	0	12	0	0	12	0
6 $\text{Isocit}^3 + \text{H}^+ \rightarrow \alpha\text{-KG}^{2-} + \text{CO}_2$	-260	260	0	0	260	0
7 $\alpha\text{-KG}^{2-} \rightarrow \text{SuccCoA}^{2-} + \text{CO}_2$	0	184	0	0	184	0
8 $\text{SuccCoA}^{2-} \rightarrow \text{Succ}^{2-}$	0	0	0	230	0	0
9 $\text{Succ}^{2-} \rightarrow \text{Fum}^{2-}$	0	0	0	0	0	294
10 $\text{Mal}^{2-} \rightarrow \text{OxAc}^{2-}$	0	0	0	0	294	0
11 $\alpha\text{-KIC} \rightarrow \text{IsoValCoA}^- + \text{CO}_2$	0	64	0	0	64	0
12 $\text{IsoValCoA}^- \rightarrow \beta\text{-MeCrotCoA}^-$	0	0	0	0	0	64
13 $\beta\text{-MeCrotCoA}^- + \text{HCO}_3^- \rightarrow \beta\text{-MeGlutcnlCoA}^{2-}$	0	0	-64	-64	0	0
14 $\text{AcAcCoA}^- + \text{CoA} \rightarrow 2 \text{AcCoA}^- + \text{H}^+$	64	0	0	0	0	0
15 $\alpha\text{-KMV}^- \rightarrow \alpha\text{-MeButCoA}^- + \text{CO}_2$	0	56	0	0	56	0
16 $\alpha\text{-MeButCoA}^- \rightarrow \text{TiglylCoA}^-$	0	0	0	0	0	56
17 $\text{TiglylCoA}^- + \alpha\text{-MeAcAcCoA}^-$	0	0	0	0	56	0
18 $\alpha\text{-MeAcAcCoA}^- + \text{CoA} \rightarrow \text{AcCoA}^- + \text{ProCoA}^- + \text{H}^+$	56	0	0	0	0	0
19 $\alpha\text{-KIV}^- \rightarrow \text{IsoButCoA}^- + \text{CO}_2$	0	54	0	0	54	0
20 $\text{IsoButCoA}^- \rightarrow \text{MeAcrylylCoA}^-$	0	0	0	0	0	54
21 $3\text{-OH-IsoBut}^- \rightarrow (S)\text{-MeMalSald}^-$	0	0	0	0	54	0
22 $(R)\text{-MeMalSald}^- \rightarrow \text{ProCoA}^- + \text{CO}_2$	0	54	0	0	54	0
23 $\text{ProCoA}^- + \text{HCO}_3^- \rightarrow (S)\text{-MeMalCoA}^{2-}$	0	0	-110	-110	0	0
24 $\text{Glu}^- \rightarrow \alpha\text{-KG}^{2-} + \text{NH}_4^+$	0	0	0	0	76	0
Totals	-140	684	-174	56	1,164	468
25 $\text{CO}_2 + \text{H}_2\text{O} \rightarrow \text{H}^+ + \text{HCO}_3^-$	140	-140	140			
Net balances	0	544	-34			
Net HCO_3^- balance of muscle			0			

Equivalent O_2 uptake	582	234
Total O_2 uptake	816	
H_{out}^+ by respiratory chain*	13,968	3,744
Total H_{out}^+ by respiratory chain	17,712	

Conventions as in Table 2. Net charge of all metabolite input to muscle cytoplasm (except bicarbonate and phosphates) is -46, whereas that of all products released from cytoplasm is -12. Net increase in charge of 34 provides a convenient check on proton plus bicarbonate balance. Corresponding values for mitochondria are -12, -46, and -34. $\alpha\text{-KIC}$, α -ketoisocaproate; IsoValCoA , isovaleryl-CoA; $\beta\text{-MeCrotCoA}$, β -methylcrotonyl-CoA; $\beta\text{-MeGlutcnlCoA}$, β -methylglutaconyl-CoA; AcAcCoA , acetoacetyl-CoA; $\alpha\text{-KMV}$, α -ketomethylvalerate; $\alpha\text{-MeButCoA}$, α -methylbutyryl-CoA; $\alpha\text{-MeAcAcCoA}$, α -methylacetoacetyl-CoA; ProCoA , propionyl-CoA; $\alpha\text{-KIV}$, α -ketoisovalerate; IsoButCoA , isobutyl-CoA; MeAcrylylCoA , methylacrylyl-CoA; 3-OH-IsoBut, 3-hydroxyisobutyrate; MeMalSald , methylmalonyl semialdehyde; MeMalCoA , methylmalonyl-CoA. For definitions of other abbreviations see Table 2. * Based on 12 protons per NADH and 8 per FPH₂.

Any lactate being produced in muscle by aerobic glycolysis or any ammonium being generated via the purine cycle is not included in our calculations. Clearly these would be separate metabolic processes simply taking place concurrently as amino acids are oxidized and for the sake of reducing the complexity of this analysis are best considered separately. We believe the overall metabolic process shown in Figure 4 is consistent with the currently available data, but we recognize the need for more studies, particularly in humans.

A. Acid-Base and Energy Balances

Proceeding in the same manner described for the gut, we have calculated the net ATP and acid-base balances associated with amino acid oxidation in skeletal muscle. As detailed in Table 5, the production and consumption of protons in muscle cells is in perfect balance. The transport of metabolites into and out of mitochondria, however, leads to the generation of 64 mmol/day bicarbonate in the matrix compartment (Table 6). An additional 12 mmol bicarbonate are formed in the matrix when the P_i^{2-} , which enters the matrix on the malate-phosphate exchanger, is protonated to form the P_i^- needed by the phosphate carrier. This association reaction is listed as *reaction 6* in Table 6 and is labeled "phosphate movement" in the overall summary of muscle bicarbonate balances shown in Figure 3, *bottom right*.

The net result of all of these events is the development of a slight excess of bicarbonate in the mitochondrial matrix compartment, 42 mmol/day. To achieve acid-base balance in the matrix, we propose that 42 mmol protons pass from the cytoplasm into the matrix via the ATP-synthetase, thereby synthesizing ~10 mmol ATP. If confirmed, such a process would constitute substrate-level ATP synthesis via chemiosmotic coupling.

With this information, the overall ATP balance can be calculated and is shown in Table 7 as ~4,500 mmol excess ATP/day.

V. EVENTS IN KIDNEY

The alanine released from the muscle passes to the liver, and some of the glutamine released is taken up by the gut, as described in section III. However, to maintain whole body acid-base balance, it is necessary for the body to generate bicarbonate metabolically, 36 mmol in the present example. Conversion of glutamine released from muscle to serine by the kidneys is thought to be the major process involved (10, 49, 61). Additional bicarbonate is generated in the kidneys by converting glycine to serine and ammonium. Because only about one-half of the NH_4^+ produced within the kidney reaches the urine, it is necessary to generate 72 mmol NH_4^+ and bicarbonate daily in the kidney to achieve whole body acid-base balance.

The metabolic process that we believe to occur in

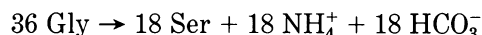
TABLE 6. Proton and charge movements associated with mitochondrial metabolite transport in muscle

Translocation Process	Type	mmol/day			
		Protons		Positive charge	
		In	Out	In	Out
1 Pyr_{in}^-/H_{in}^+	Symport	12			
2 $Asp_{out}^-/Glu_{in}^- \cdot H_{in}^+$	Antiport	34		34	
3 Glu_{out}^-/H_{out}^+	Symport		98		
4 $\alpha\text{-KG}_{out}^{2-}/Mal_{in}^{2-}$ (12)	Antiport				
5 $Mal_{out}^{2-}/P_{i,in}^{2-}$ (12)	Antiport				
6 $P_{i,in}^{2-} + H^+ \rightarrow P_{i,in}^-$ (12)	*				
7 $P_{i,out}^-/H_{out}^+$	Symport†		12		
8 BCAA (174)	Neutral, entry				
Totals		46	110	34	0
Net			64	34	

$$\begin{aligned} \text{ATP cost of translocation} &= (-64) \times \frac{1}{16} + 34 \times \frac{3}{16} \\ &= -4 + 6\frac{3}{8} \approx 2 \end{aligned}$$

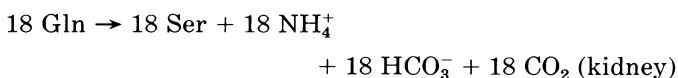
Calculations are as in Table 3. Numbers in parentheses are millimoles per day of substances transported without obligatory proton or charge movements. BCAA, branched-chain amino acids. For definitions of other abbreviations see Table 2. * This reaction occurs in mitochondrial matrix and is the result of ionic specificities of transporters involving P_i . It is shown in Fig. 3 as "phosphate movement" but has been omitted from the metabolic maps. The reverse reaction occurs in the cytoplasm. † Translocation shown as a $P_i^- \cdot H^+$ symport may include a $P_i^{2-} \cdot 2H^+$ symport as well. This would not influence our analysis as long as the phosphate movement is adjusted correspondingly.

the kidneys is outlined in Figure 5, with a more detailed scheme shown in Figure 10 of APPENDIX B. The process consists of the following three reactions



Because acidosis is not present, we assume that the kidneys convert negligible amounts of glutamine to glucose (61). It should be added that although this total kidney serine production of 54 mmol/day accords with the experimental data (10), the actual precursors are not yet clearly established. It is known that glycine and glutamine are the major amino acids consumed by the kidneys under these conditions (45, 57, 62).

Figure 5 shows that there are 36 mmol NH_4^+ (accompanied by 72 mmol HCO_3^-) that reach the renal vein and thus the liver, where it and one-half of the HCO_3^- reaching the renal vein is recombined to form urea and CO_2 . Note that no net bicarbonate production results when ammoniogenesis is followed by ureagenesis. Consider the reactions involved for the one-half of the NH_4^+ produced in the kidney that reaches the liver



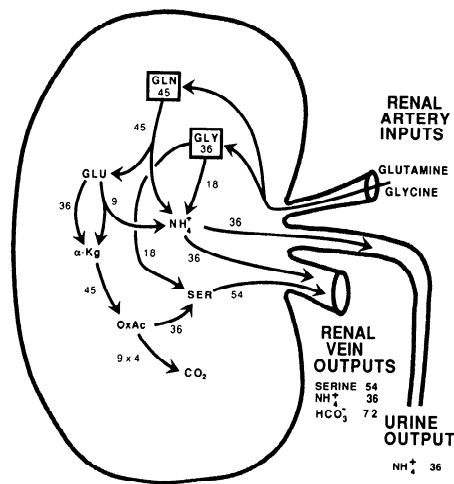
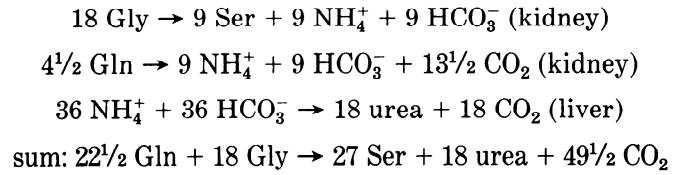


FIG. 5. Metabolic process occurring in kidneys during oxidation of daily supply of amino acids in humans. Two amino acids supplied to kidneys are enclosed in boxes, glycine coming from diet and glutamine mainly from muscle. Net amount of product formed in each step (in mmol/day) is indicated by number associated with each arrow. See Fig. 10 in APPENDIX B for more complete portrayal. For definitions of abbreviations see Fig. 1.



The major acid-base significance of ammonium excretion is that it prevents the fourth reaction listed above from occurring, i.e., it prevents liver ureagenesis from consuming the bicarbonate generated by kidney ammoniogenesis, thereby ensuring a net metabolic bicarbonate production.

TABLE 7. Calculation of the ATP balance in muscle

	mmol/day	
Total H _{out} ⁺ respiratory chain (Table 5)	17,712	
H _{out} ⁺ by substrate-level metabolism (Fig. 3)	42	
Total H _{out} ⁺ available for oxidative phosphorylation	17,754	
Net mitochondrial ATP from amino acids*	446	446
Mitochondrial ATP made at substrate level (Table 5)	56	
Mitochondrial ATP made by oxidative phosphorylation	390	
H _{in} ⁺ used to make mitochondrial ATP (×3)	1,170	
Remaining H _{in} ⁺ balance	16,584	
Cytoplasmic ATP by oxidative phosphorylation (÷4)	4,146	
Cytoplasmic ATP at substrate level (Table 5)	-76	
Cytoplasmic ATP used to transport positive charge (Table 6)†	-6	
Cytoplasmic ATP used for amino acid transport‡	-58	
Net cytoplasmic ATP from amino acids	4,006	4,006
Net ATP balance of muscle		4,452

* It was assumed that the consumption of ATP by reactions external to amino acid oxidation process was 90% cytoplasmic and 10% mitochondrial. That is, of 4,452 mmol ATP made available to muscle each day as a result of amino acid oxidation, 446 mmol were assumed to be utilized in mitochondrial matrix. † Only ATP cost of transporting positive charge is included because movement of protons has already been included in adjustment for substrate level metabolism. ‡ Cost of amino acid transport was calculated on the assumption that a branched-chain amino acid is taken into muscle cells via a symport mechanism along with 1 Na⁺. Each Na⁺ was considered equivalent to 1/3 of a cytoplasmic ATP.

A. Acid-Base and Energy Balances

The balances of ATP and bicarbonate for the process occurring in the kidneys are shown in Table 8. The metabolic reactions lead to the generation of 72 mmol/day of bicarbonate equally divided between cytoplasm and mitochondria. Metabolite transport exactly neutralizes the balance in the matrix compartment (Table 9), leaving the bicarbonate excess all in the cytoplasm (Fig. 3, bottom middle). Thus no uncoupled respiration is required for acid-base balance. The ATP balance is ~700 mmol/day (Table 10).

VI. EVENTS IN LIVER

We next turn our attention to the liver. Two central processes dominate the metabolic events in liver during amino acid oxidation-gluconeogenesis and ureagenesis. Each involves the interaction of mitochondrial and cytoplasmic events. Together they form a complex metabolic process that can be viewed as generating as major products only glucose (or glycogen), urea, and CO₂. The net effect of the overall process is to convert a group of specialized fuels, the amino acids, which for the most part cannot be rapidly oxidized in any other organ, into a universal fuel, glucose. The process is self-sufficient energetically despite the ATP requirements for synthesizing glucose and urea. The most useful outcome is that the majority of the energy supplied as dietary protein is made available to all tissues of the body without the need for each to synthesize a complex array of amino acid-metabolizing enzymes. For simplicity, we ignore the fact that a small portion of some of the amino acids are used by the liver as precursors for the biosynthesis of a variety of essential cofactors and amines.

TABLE 8. Balance of ATP, CO₂, and HCO₃⁻ in kidney

Reactions in Cytoplasm	mmol/day					
	H ⁺	CO ₂	HCO ₃ ⁻	ATP	NADH	FPH ₂
1 OxAc ²⁻ + H ⁺ → PEP ⁻ + CO ₂	-36	36	0	-36	0	0
2 3-PGA ⁻ → 3-P-OH-Pyr ⁻	0	0	0	0	36	0
3 OxAc ²⁻ → Mal ²⁻	0	0	0	0	-36	0
Totals	-36	36	0	-36	0	0
4 CO ₂ + H ₂ O → H ⁺ + HCO ₃ ⁻	36	-36	36	0	0	0
Net balances	0	0	36	-36	0	0

Reactions in mitochondria	mmol/day					
	H ⁺	CO ₂	HCO ₃ ⁻	ATP	NADH	FPH ₂
5 Pyr → AcCoA ⁻ + CO ₂	0	9	0	0	9	0
6 Isocit ³⁻ + H ⁺ → α-KG ²⁻ + CO ₂	-9	9	0	0	9	0
7 α-KG ²⁻ → SuccCoA ²⁻ + CO ₂	0	54	0	0	54	0
8 SuccCoA ²⁻ → Succ ²⁻	0	0	0	54	0	0
9 Succ ²⁻ → Fum ²⁻	0	0	0	0	0	54
10 Mal ²⁻ → OxAc ²⁻	0	0	0	0	81	0
11 Mal ²⁻ + H ⁺ → Pyr ⁻ + CO ₂	-9	9	0	0	9	0
12 Glu ⁻ → α-KG ²⁻ + NH ₄ ⁺	0	0	0	0	9	0
13 Gly + FH ₄ + H ⁺ → NH ₄ ⁺ + CO ₂ + CH ₂ FH ₄	-18	18	0	0	18	0
Totals	-36	99	0	54	189	54
14 CO ₂ + H ₂ O → H ⁺ + HCO ₃ ⁻	36	-36	36			
Net balances	0	63	36			
Net HCO ₃ ⁻ balance of kidney			72			

Equivalent O ₂ uptake	94½	27
Total O ₂ uptake	121½	
H _{out} ⁺ by respiratory chain*	2,268	432
Total H _{out} ⁺ by respiratory chain	2,700	

Conventions as in Table 2. Net charge of all metabolites input to kidney cytoplasm (except bicarbonate and phosphates) is -144, whereas that of all products released is -108, giving a net increase in charge of 36. Corresponding values for mitochondria are -108, -144, and +36. These numbers provide a convenient check on the proton plus bicarbonate balances. FH₄, tetrahydrofolate; CH₂FH₄, methylenetetrahydrofolate. For definitions of other abbreviations see Table 2. * Based on 12 protons per NADH and 8 per FPH₂.

Because of the processing of some of the dietary amino acids by the gut, muscle, and kidney, the amino acid inputs to the liver differ substantially from the dietary inputs (Table 11). In our example the supply of alanine is more than tripled and that of serine is doubled, whereas six amino acids are completely or largely metabolized elsewhere. Also shown in Table 11 as a carbon input is the lactate produced from amino acids in the gut and the ammonium derived from the gut and kidney. The products calculated to be released daily by the liver include 439.5 mmol glucose, 864 mmol urea, 3 mmol acetoacetate, 36 mmol sulfate, and 12 mmol creatine, while 640 mmol bicarbonate are consumed to maintain acid-base balance.

Figure 6 summarizes the essential features of the enormously complex metabolic process occurring in the liver, with the more complete version presented in Figure 11 of APPENDIX B. Even Figure 6 is extremely complex, and we beg the readers' indulgence. Further simplifying of the drawing obscures important features that we consider essential to a full understanding of the metabolic process.

TABLE 9. Proton and charge movements associated with mitochondrial metabolite transport in kidney

Translocation Process	Type	mmol/day			
		Protons		Positive charge	
		In	Out	In	Out
1 Asp _{out} ⁻ /Glu _{in} ⁻ · H _{in} ⁺	Antiport	72		72	
2 Glu _{out} ²⁻ /H _{out} ⁺	Symport		36		
3 α-KG _{out} ²⁻ /Mal _{in} ²⁻ (36)	Antiport				
4 Ser _{out} (18)	Neutral exit?				
5 NH ₄ _{out} ⁺	*				72
Totals		72	36	72	72
Net		36		0	

ATP cost of translocation = 36 × 1/16 + 0 × 3/16 ≈ 2

Movements of protons or positive charge into or out of kidney mitochondria. Numbers in parentheses are millimoles per day of substances transported without obligatory proton or charge movements. ATP costs of metabolite transport estimated as in Table 3. Mechanism involved in the translocation of serine remains unclear; no proton movement was invoked. For definitions of abbreviations see Table 2. * Conventions as in Table 3.

TABLE 10. *Calculation of the ATP balance in kidneys*

	mmol/day	
Total H_{out}^+ respiratory chain (Table 8)	2,700	
H_{out}^+ by uncoupled respiration (Fig. 3)	0	
Total H_{out}^+ available for oxidative phosphorylation	2,700	
Net mitochondrial ATP from amino acids*	66	66
Mitochondrial ATP made at substrate level (Table 8)	54	
Mitochondrial ATP made by oxidative phosphorylation	12	
H_{in}^+ used to make mitochondrial ATP ($\times 3$)	36	
Remaining H_{in}^+ balance	2,664	
Cytoplasmic ATP by oxidative phosphorylation ($\div 4$)	666	
Cytoplasmic ATP at substrate level (Table 8)	-36	
Cytoplasmic ATP used to transport positive charge (Table 9)†	-0	
Cytoplasmic ATP used for amino acid transport‡	-27	
Net cytoplasmic ATP from amino acids	603	603
Net ATP balance of kidneys		669

* It was assumed that the consumption of ATP by reactions external to amino acid oxidation process was 90% cytoplasmic and 10% mitochondrial. That is, of 669 mmol ATP made available to kidneys each day as a result of amino acid oxidation, 66 mmol were assumed to be utilized in the mitochondrial matrix. † Only the ATP cost of transporting positive charge is included because the movement of protons has already been included in the adjustment for uncoupled respiration. ‡ Cost of amino acid transport was calculated on the assumption that glutamine and glycine are taken into cells via a symport mechanism along with 1 Na^+ . Each Na^+ was considered equivalent to $\frac{1}{3}$ of a cytoplasmic ATP.

With a process as complex as this, calculation of the daily net flux through each step can be quite complicated, for example, at the step from mitochondrial oxaloacetate to aspartate. It is intuitively evident that if the flow from each of the 18 inputs to the liver is fixed and

all pathways are known, the net flux through each metabolic step must also be fixed. A systematic approach is possible, but it requires the solution of very many simultaneous equations. The process is too complex for trial and error methods to be efficient. The approach we found most effective is described in APPENDIX A.

TABLE 11. *Liver inputs and outputs*

Amino Acids	mmol/day						
	Input source					Outputs	
	Diet	Gut	Muscle	Kidney	Total	Product	Total
Alanine	78	177	22		277	Urea	864
Aspartate	38	−38			0	Glucose	439½
Asparagine	62				62	Sulfate	36
Arginine	46				46	Creatine	12
Cysteine	12				12	Acetoacetate	39
Glutamine	56	−69	76	−45	18		
Glutamate	70	−70			0		
Glycine	98			−36	62		
Histidine	30				30		
Lysine	76				76		
Leucine	84		−64		20		
Isoleucine	56		−56		0		
Methionine	24				24		
Phenylalanine	32				32		
Proline	52				52		
Serine	50			54	104		
Threonine	48				48		
Tryptophan	8				8		
Tyrosine	26				26		
Valine	54		−54		0		
Totals	1,000	0	−76	−27	897		
Others							
Lactate		114			114		
NH ₄ ⁺		469		36	505		
HCO ₃ [−] consumed					640		

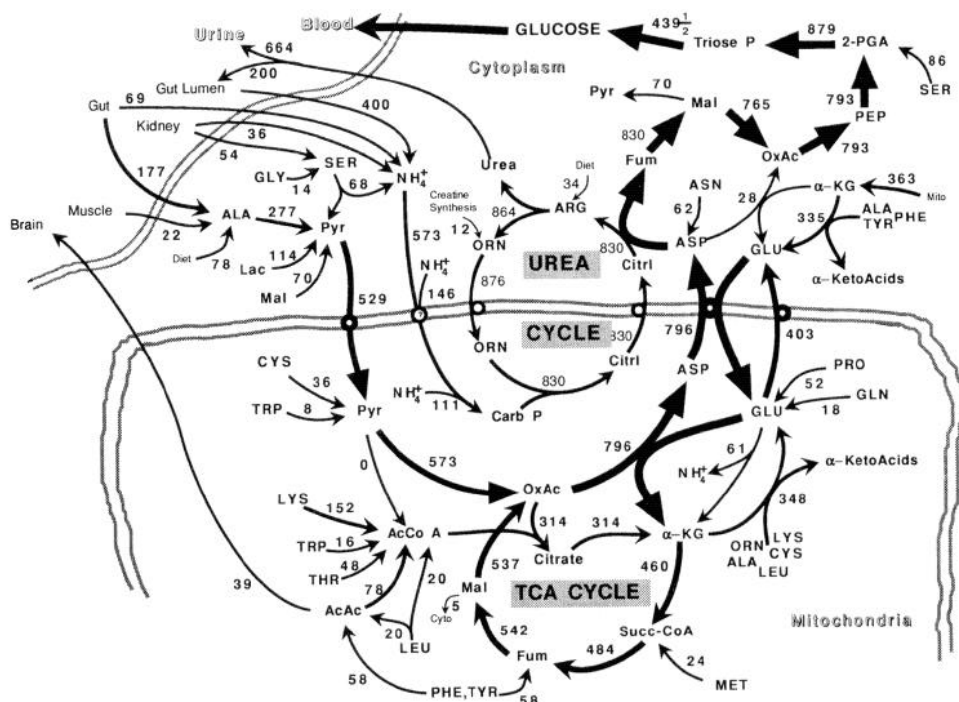
A. Assumptions

To make the problem manageable we made the following major assumptions.

1) The major fuel into which the amino acid carbon is converted is glucose. Small quantities of acetoacetate are also generated, some of which is released from the liver as discussed in section XI. Under some conditions substantial quantities of amino acid carbon could be converted by the liver to triglycerides and released to the periphery as very low-density lipoproteins. The whole body indirect calorimetry studies of Acheson et al. (1) reveal, however, how unusual it is for net fat synthesis to exceed net fat oxidation in humans even after carbohydrate loading. In fact, most of the conclusions drawn here would not be altered were fat also a major biosynthetic product, although the complexity of the discussion would be much greater.

2) We ignore most other metabolic events occurring in liver that need not be associated directly with amino acid oxidation. For example, fatty acid oxidation is neglected, and no pyruvate is allowed to flow to acetyl-CoA and thus on to CO_2 . We did this to allow a calculation of the energy yield inherent in processing a physiological mixture of amino acids to glucose. Certainly under normal circumstances both carbohydrate and fat would be undergoing some oxidation at the same time as the

FIG. 6. Metabolic process occurring in liver during oxidation of daily supply of amino acids in humans. Heavy stippled lines represent inner mitochondrial membrane, and lighter stippled line represents hepatocyte plasma membrane. Numbers near each arrow designate amount of amino acid input or net amount of product formed in each step (in mmol/day). Circles in inner membrane represent substrate transporters. For convenience, conversion of acetoacetate to acetoacetyl-CoA is shown in mitochondrial sector even though synthetase involved is a cytoplasmic enzyme. Carb P, carbamoyl phosphate; Citrl, citrulline; cyto, cytoplasm; Fum, fumarate; Mal, malate; PEP, phosphoenolpyruvate; mito, mitochondria; 2-PGA, 2-phosphoglycerate; triose P, triose phosphate. For definitions of other abbreviations see Fig. 1.



amino acids. Our intent is to separate out these metabolic processes into separate balanced processes that can later be recombined by simple addition to gain a picture of the total metabolism of the hepatic cell. Similarly, concurrent gluconeogenesis from glycerol derived from fat metabolism or from lactate undergoing the Cori cycle has been omitted. We also set cholesterol synthesis from acetoacetate to zero even though a significant fraction of this intermediate may normally be converted to cholesterol (8).

3) One exception is creatine synthesis. To maintain a steady state, creatine must be synthesized in liver at a rate of 12 mmol/day at the expense of arginine, glycine, and methionine. This just balances the daily nonenzymatic conversion of creatine to creatinine, mainly in muscle, and constitutes a quantitatively significant aspect of whole body amino acid metabolism that we do not want to ignore.

4) The metabolic pathway utilized for the oxidation of some amino acids remains unclear.² In general when a

choice had to be made, the pathway was chosen that maximized the production of glucose or ATP.

5) Cytoplasmic generation and consumption of NADH and NADPH must be in balance. The latter is required for the hydroxylation of phenylalanine to tyrosine and for the reduction of both N^5,N^{10} -methenyl-FH₄ and N^{10} -formyl-FH₄ to N^5,N^{10} -methylene-FH₄. It was generated entirely via the malate cycle for simplicity. This required translocating a very small amount of malate from the mitochondria to the cytoplasm, returning it as pyruvate (see Fig. 11 in APPENDIX B). To maintain NADH balance a small fraction of cytoplasmic aspartate had to be directly transaminated to oxaloacetate.

6) We ignore the possible role of intramitochondrial phosphoenolpyruvate (PEP) carboxykinase (see sect. XII). Carbon was allowed to exit the mitochondria only as citrulline, aspartate, malate, glutamate, or α -ketoglutarate.

B. Pathway of Carbon and Nitrogen Flow

The metabolic process summarized in Figure 6 is now briefly described. Near the center is the urea cycle, shown occurring partly outside the mitochondrial inner membrane and partly within. Only 34 of the 46 mmol arginine consumed per day are considered to enter the urea cycle directly. The remaining 12 mmol are involved in creatine synthesis and thus enter the cycle only after conversion to cytoplasmic ornithine. Thus in our example 46 mmol of urea cycle intermediates are generated daily from dietary arginine and must exit from the cycle if a steady state is to be maintained. This exit is accomplished by the conversion of 46 mmol of mitochondrial

² After accounting for creatine synthesis there remain 12 mmol methionine to be oxidized. We assume that the methyl group is oxidized via mitochondrial sarcosine dehydrogenase to N^5,N^{10} -methylene tetrahydrofolate. One-carbon fragments generated from the oxidation of histidine and tryptophan are assumed to arrive at this same intermediate. From there the carbon is transferred to glycine to form serine, which is converted to pyruvate by cytosolic serine dehydratase. Dietary serine and that generated in the mitochondria from threonine are processed via mitochondrial serine aminotransferase to hydroxypyruvate. In this way total liver serine metabolism is split approximately equally between the serine dehydratase and serine aminotransferase pathways (56). Threonine is assumed to be processed in mitochondria via threonine dehydrogenase and 2-amino-3-ketobutyrate ligase to glycine and acetyl-CoA (9). The mitochondrial glycine so generated is oxidized via the glycine dehydrogenase complex and mitochondrial serine hydroxymethyl transferase to serine.

ornithine to glutamate (omitted from Fig. 6, see Fig. 11 in APPENDIX B). By far the greatest share of mitochondrial ornithine reacts with carbamoyl phosphate to generate citrulline (830 mmol). Citrulline exits the mitochondria and is converted to arginine in the cytoplasm. When added to the 34 mmol arginine obtained from the diet, this provides the 864 mmol arginine cleaved by arginase each day.

Not all of the urea secreted by the liver reaches the urine; about one-quarter instead diffuses into the lumen of the colon where bacterial ureases cleave it to ammonium and bicarbonate, which are reabsorbed (7). We somewhat arbitrarily assigned 200 mmol/day (23%) of the urea produced to this cycling process. Thus the colon lumen becomes the largest supplier of the ammonium used for ureagenesis; in our example, 400 mmol would be generated by bacterial ureases. The effect of variations in the amount of urea recycling on the overall metabolic process occurring is discussed in section XIII.

Additional NH_4^+ is supplied by the metabolic reactions occurring in the intestinal mucosal cells and by the kidneys, as described in sections III and V. All of the remaining ammonium used for ureagenesis is produced within the liver: 214 mmol are generated by cytoplasmic deaminases while 111 arise from within the mitochondria (Fig. 6). Immediately we see the paradox. Less than 15% of the 830 mmol ammonium used for carbamoyl phosphate synthesis arises within the mitochondrial matrix; the remainder either reaches the liver cell via the cytoplasm or is directly generated in that compartment. However, the cell has chosen to fix the site where this toxic substance is consumed as the mitochondrial matrix. Could this be explained by the observation that the true substrate for carbamoyl phosphate synthesis is the unprotonated species, NH_3 , and the fact that the matrix space is ~ 0.8 pH units more alkaline than the cytoplasm because of the operation of the respiratory chain proton pump? Much depends on the accuracy of the widely held assumption that NH_3 passes the inner mitochondrial membrane freely and thus is equal in concentration on both sides. We discuss this point in section XIV in more detail.

We turn next to a consideration of the main flow of carbon from amino acids to glucose as shown by the heavy arrows in Figure 6. This flow starts at the top left with 177 mmol alanine released from the gut. The supply of alanine is enlarged by the 78 mmol in the diet and 22 mmol released from skeletal muscle, giving a total of 277 mmol alanine flowing to pyruvate. Another 68 mmol pyruvate are formed from serine produced either by the kidneys or within the liver cytoplasm from glycine. An additional 70 mmol pyruvate are produced by the malate cycle, and 114 mmol more derive from lactate.

The resulting 529 mmol pyruvate are actively transported into the mitochondrial matrix together with a proton. There the flow is joined by 36 mmol pyruvate formed from the sulfur-containing amino acids and 8 mmol formed from tryptophan. A critical branch point in pyruvate metabolism is now reached. As pointed out, we assume that all 573 mmol pyruvate undergo carboxyl-

ation to form oxaloacetate and thus take the branch leading to gluconeogenesis, and none are decarboxylated to acetyl-CoA. In fact a small amount of pyruvate undoubtedly is oxidized to acetyl-CoA and thus flows either to fat or on to CO_2 . However, the metabolic conditions existing in the liver during amino acid oxidation (see sect. IX) most likely keep the pyruvate dehydrogenase activity at a low level.

The main flow of carbon proceeds from oxaloacetate to aspartate, utilizing the dominant mitochondrial aminotransferase involving glutamate. Flow at this step is increased to 796 mmol/day as amino acid carbon entering the main flow at the level of the tricarboxylic acid cycle joins in. Only 5 mmol or $\sim 1\%$ of the malate feeding into the oxaloacetate pool exits directly to the cytoplasm.

The bulk of the mitochondrial aspartate formed is actively transported out of the matrix by an exchange carrier that links aspartate exit with the entry of glutamate and a proton. As shown in Figure 6, about one-half of the glutamate entering the matrix in this way simply recycles back to the cytoplasm via a different specific glutamate carrier.

There are two possible fates for cytoplasmic aspartate, but except under unusual circumstances it is clear that the bulk of the aspartate formed from amino acid carbon must react with citrulline to form arginine and fumarate. In our example we have 796 mmol aspartate exiting the mitochondria to which are added the 62 mmol generated in the cytoplasm by deamination of asparagine. Under the circumstances of our example the second possible fate of aspartate, transamination to oxaloacetate, amounts to only 28 mmol/day or 3% of the cytoplasmic aspartate turnover. A very important point emerges. The metabolite flows through the two major pathways, gluconeogenesis and ureagenesis, are interlinked because they share a common step. The significance of this linkage is discussed in section XII.

The main flow of carbon to glucose is completed via well-known steps. After hydration of fumarate to malate the flow is joined by the 5 mmol malate exiting from the mitochondria (omitted from Fig. 6). Exactly 70 mmol of cytoplasmic malate must flow to pyruvate to maintain cytoplasmic NADPH balance. To maintain cytoplasmic NADH balance, the 765 mmol oxaloacetate produced by the oxidation of malate must be joined by 28 mmol produced by the transamination of aspartate. There are 86 mmol 2-phosphoglycerate generated in the mitochondria from serine and threonine that must be reduced to triose phosphate in the cytoplasm so that a total of 879 mmol NADH are required by glyceraldehyde phosphate dehydrogenase. The supply of NADH from lactate oxidation is 114 mmol, so 765 mmol must arise from malate dehydrogenase.

For simplicity, we set the recycling of PEP back to pyruvate to zero, although it undoubtedly does occur (13a, 36, 53). The result is that all 793 mmol of cytoplasmic PEP arrive at glucose. The yield of glucose is thus one-half of 793 plus one-half of 86 or 439.5 mmol/day. Subtracting the 88.5 mmol used by the intestine to gener-

ate alanine, we have a net yield of 351 mmol or 63.2 g glucose. As 1,328 mmol nitrogen appear as urinary urea during this overall process, the ratio of grams of glucose formed to grams of urea nitrogen is 3.40. If we include the 36 mmol of urinary ammonium and 36 mmol of urinary creatinine nitrogen, this ratio becomes 3.22 g glucose/g urinary nitrogen. Because 110 g protein were oxidized (see Table 1), it follows that 57 g glucose result from the oxidation of 100 g dietary protein. About a 10% larger yield of glucose would be expected from protein mobilized during fasting, as less glutamate and aspartate would be oxidized to CO_2 in the gut.

C. Acid-Base and Energy Balances

The acid-base and ATP balances of the metabolic reactions occurring in liver cytoplasm as the amino acids are converted to glucose are shown in Table 12. Notice that there is a large net production of bicarbonate amounting to >1,700 mmol/day. The conversion of aspartate carbon to glucose of course requires large amounts of ATP, and in this example the need is ~3.5 mol daily.

Similar calculations for the liver mitochondria are

summarized in Table 13. In this case there is a net consumption of large quantities of bicarbonate, in our example well over 2 mol/day. The large ATP requirements for bicarbonate fixation into oxaloacetate and urea exceed the production of ATP at the substrate level, so there is also a need in the matrix for ATP generated by oxidative phosphorylation.

The multiple metabolite transport steps involved in this complex process are shown in Table 14 along with their acid-base and energetic consequences. The translocations across the inner mitochondrial membrane are driven by the net inward movement of ~0.5 mol protons and 2.5 equivalents of positive charge daily and in the aggregate cost the equivalent of just over 500 mmol ATP. As summarized in Figure 3 (*top right*), the combined effect of the metabolic reactions and the metabolite transport steps is the generation of an enormous bicarbonate deficit within the matrix, nearly 3 mol daily. Only a small fraction of this deficit can be met by the protonation of P_i^{2-} entering on the malate antiport to form the P_i^- that exits on the phosphate carrier (labeled "phosphate movement" in Figure 3, it amounts to 368 mmol/day). Consequently, there is a major need for proton extrusion via the respiratory chain to achieve

TABLE 12. Balance of ATP, CO_2 , and HCO_3^- in liver cytoplasm

Reaction	mmol/day						
	H^+	CO_2	HCO_3^-	ATP	NADH	NADPH	O_2
1 $\text{OxAc}^{2-} + \text{H}^+ \rightarrow \text{PEP}^- + \text{CO}_2$	-793	793	0	-793	0	0	0
2 $3\text{-PGA}^- \rightarrow 1,3\text{-BPG}^-$	0	0	0	-879	0	0	0
3 $1,3\text{-BPG}^- + \text{H}^+ \rightarrow \text{GAP}$	-879	0	0	0	-879	0	0
4 $\text{Asp}^- + \text{Citrl} \rightarrow \text{Arg}^+ + \text{Fum}^{2-}$	0	0	0	-830	0	0	0
5 $\text{AMP} \rightarrow \text{ADP}$	0	0	0	-893	0	0	0
6 $\text{Mal}^{2-} \rightarrow \text{OxAc}^{2-}$	0	0	0	0	765	0	0
7 $\text{Mal}^{2-} + \text{H}^+ \rightarrow \text{Pyr}^- + \text{CO}_2$	-70	70	0	0	0	70	0
8 $\text{AcAc}^- + \text{CoA} \rightarrow \text{AcAcCoA}^-$	0	0	0	-39	0	0	0
9 $\text{AcAcCoA}^- + \text{CoA} \rightarrow 2 \text{AcCoA}^- + \text{H}^+$	39	0	0	0	0	0	0
10 $\text{Lac}^- \rightarrow \text{Pyr}^-$	0	0	0	0	114	0	0
11 $\text{Uro} + \text{H}_2\text{O} \rightarrow 4\text{-Im-5-Pro}^- + \text{H}^+$	16*	0	0	0	0	0	0
12 $4\text{-Im-5-Pro}^- + \text{H}_2\text{O} \rightarrow N\text{-ForImGlu}^{2-} + \text{H}^+$	30	0	0	0	0	0	0
13 $N\text{-ForImGlu}^{2-} + \text{FH}_4 + \text{H}^+ \rightarrow N^5\text{-ForImFH}_4 + \text{Glu}^-$	-30	0	0	0	0	0	0
14 $N^5\text{-ForImFH}_4 + \text{H}^+ \rightarrow N^5, N^{10}\text{-CH-FH}_4 + \text{NH}_4^+$	-30	0	0	0	0	0	0
15 $N^5, N^{10}\text{-CH-FH}_4 \rightarrow N^5, N^{10}\text{-CH}_2\text{-FH}_4$	0	0	0	0	0	-30	0
16 $\text{Trp} + \text{O}_2 + \text{H}_2\text{O} \rightarrow \text{Kyn} + \text{For}^- + \text{H}^+$	8	0	0	0	0	0	-8
17 $\text{For}^- + \text{FH}_4 + \text{H}^+ \rightarrow N^{10}\text{-For-FH}_4$	-8	0	0	-8	0	0	0
18 $N^{10}\text{-For-FH}_4 \rightarrow N^5, N^{10}\text{-CH}_2\text{-FH}_4$	0	0	0	0	0	-8	0
19 $\text{Phe} + \text{O}_2 \rightarrow \text{Tyr}$	0	0	0	0	0	-32	-32
20 $\text{Met} + \text{H}^+ \rightarrow \text{SAM}^+$	-24	0	0	-24	0	0	0
21 $\text{SAM}^+ + \text{Gly} \rightarrow \text{Sarc} + \text{SAH} + \text{H}^+$	12	0	0	0	0	0	0
22 $\text{SAM}^+ + \text{GuAc} \rightarrow \text{creatine} + \text{SAH} + \text{H}^+$	12	0	0	0	0	0	0
23 $\text{Adenosine} \rightarrow \text{AMP}$	0	0	0	-24	0	0	0
Totals	-1,717	863	0	-3,490	0	0	-40
24 $\text{CO}_2 + \text{H}_2\text{O} \rightarrow \text{H}^+ + \text{HCO}_3^-$	1,717	-1,717	1,717				
Net balances	0	-854	1,717				

Conventions as in Table 2. Net charge of all metabolite input to cytoplasm (except phosphates and bicarbonate) is -2,184, whereas that of all products released from the cytoplasm is -467. Net increase in charge of 1,717 provides a convenient check on the proton plus bicarbonate balance. Citrl, citrulline; AcAc, acetoacetate; AcAcCoA, acetoacetyl-CoA; Uro, urocanic acid; 4-Im-5-Pro, 4-imidazolone-5-propionate; N-ForImGlu, N-formimino glutamate; FH_4 , tetrahydrofolate; $N^5\text{-ForImFH}_4$, N^5 -formiminotetrahydrofolate; $N^5, N^{10}\text{-CH-FH}_4$, N^5, N^{10} -methenyltetrahydrofolate; $N^5, N^{10}\text{-CH}_2\text{-FH}_4$, N^5, N^{10} -methylene tetrahydrofolate; Kyn, kynurenine; For, formate; $N^{10}\text{-For-FH}_4$, N^{10} -formyltetrahydrofolate; SAM, (S)-adenosylmethionine; Sarc, sarcosine; SAH, (S)-adenosylhomocysteine; GuAc, guanidinoacetate. For definitions of other abbreviations see Table 2. * At the pH of the cytoplasm only 16 of 30 mmol histidine that undergo metabolism carry the proton on imidazole ring nitrogen, which is released when urocanate is hydrated to 4-imidazolone-5-propionate.

TABLE 13. Balance of ATP, CO₂, and HCO₃⁻ in liver mitochondria

Reaction	mmol/day								
	H ⁺	CO ₂	HCO ₃ ⁻	ATP	NADH	NADPH	FPH ₂	Cyt c	O ₂
1 Pyr ²⁻ + HCO ₃ ⁻ → OxAc ²⁻	0	0	-573	-573	0	0	0	0	0
2 Isocit ³⁻ + H ⁺ → α-KG ²⁻ + CO ₂	-314	314	0	0	314	0	0	0	0
3 α-KG ²⁻ → SuccCoA ²⁻ + CO ₂	0	460	0	0	460	0	0	0	0
4 SuccCoA ²⁻ → Succ ²⁻	0	0	0	484	0	0	0	0	0
5 Succ ²⁻ → Fum ²⁻	0	0	0	0	0	0	484	0	0
6 Mal ²⁻ → OxAc ²⁻	0	0	0	0	537	0	0	0	0
7 NH ₄ ⁺ + HCO ₃ ⁻ → CarbP ⁻ + H ⁺	830	0	-830	-1,660	0	0	0	0	0
8 Glu ⁻ → α-KG ²⁻ + NH ₄ ⁺	0	0	0	0	61	0	0	0	0
9 α-KBut ⁻ + CoA → ProCoA ⁻ + CO ₂	0	24	0	0	24	0	0	0	0
10 ProCoA ⁻ + HCO ₃ ⁻ → (S)-MeMalCoA ²⁻	0	0	-24	-24	0	0	0	0	0
11 Sarc + FH ₄ → Gly + CH ₂ -FH ₄	0	0	0	0	0	0	12	0	0
12 Thr → α-Am-β-Oxo-But ⁻	0	0	0	0	48	0	0	0	0
13 α-Am-β-Oxo-But ⁻ + CoA → Gly + AcCoA ⁻ + H ⁺	48	0	0	0	0	0	0	0	0
14 Gly + FH ₄ + H ⁺ → CH ₂ -FH ₄ + CO ₂ + NH ₄ ⁺	-24	24	0	0	24	0	0	0	0
15 OH-Pyr ⁻ → glycerate ⁻	0	0	0	0	-86	0	0	0	0
16 Glycerate ⁻ → 2-PGA ⁻	0	0	0	-86	0	0	0	0	0
17 Cys + 2 O ₂ → CysSulfin ⁻ + H ⁺	36	0	0	0	-72	0	0	0	-72
18 Sulfinpyr ²⁻ + H ⁺ → Pyr ⁻ + SO ₂	-36	0	0	0	0	0	0	0	0
19 SO ₂ + H ₂ O → SO ₃ ²⁻ + 2 H ⁺	72	0	0	0	0	0	0	0	0
20 SO ₃ ²⁻ + 2 Cyto c ³⁺ → SO ₄ ²⁻ + 2 Cyto c ²⁺	0	0	0	0	0	0	0	72	0
21 Kyn + O ₂ → 3-OH-Kyn	0	0	0	0	0	-8	0	0	-8
22 3-OH-Kyn → Ala + 3-OH-Anthr ⁻ + H ⁺	8	0	0	0	0	0	0	0	0
23 3-OH-Anthr ⁻ + O ₂ → α-Am-β-CarbMucSald ⁻	0	0	0	0	0	0	0	0	-8
24 α-Am-β-CarbMucSald ⁻ + H ⁺ → CO ₂ + α-Am-MucSald	-8	8	0	0	0	0	0	0	0
25 α-Am-MucSald → α-Am-Muc ⁻ + H ⁺	8	0	0	0	8	0	0	0	0
26 α-Am-Muc ⁻ → α-KAdip ²⁻ + NH ₄ ⁺	0	0	0	0	0	-8	0	0	0
27 Lys ⁺ + α-KG ²⁻ → Sacchar ²⁻ + H ⁺	76	0	0	0	0	-76	0	0	0
28 Sacchar ²⁻ + H ⁺ → Glu ⁻ α-AmAdipSald	-76	0	0	0	76	0	0	0	0
29 α-AmAdipSald → α-AmAdip ⁻ + H ⁺	76	0	0	0	0	76	0	0	0
30 α-KAdip ²⁻ + CoA → GlutrylCoA ²⁻ + CO ₂	0	84	0	0	84	0	0	0	0
31 GlutrylCoA ²⁻ → GlutnCoA ²⁻	0	0	0	0	0	0	84	0	0
32 GlutnCoA ²⁻ + H ⁺ → CrotCoA ⁻ + CO ₂	-84	84	0	0	0	0	0	0	0
33 β-OH-ButCoA ⁻ → AcAcCoA ⁻	0	0	0	0	84	0	0	0	0
34 AcAc-CoA ⁻ + CoA → 2 AcCoA ⁻ + H ⁺	84	0	0	0	0	0	0	0	0
35 α-KIC ⁻ → IsoValCoA ⁻ + CO ₂	0	20	0	0	20	0	0	0	0
36 IsoValCoA ⁻ → β-MeCrotCoA	0	0	0	0	0	0	20	0	0
37 β-MeCrotCoA ⁻ + HCO ₃ ⁻ → β-MeGlutnCoA ²⁻	0	0	-20	-20	0	0	0	0	0
38 p-OH-Φ-Pyr ⁻ + O ₂ → Homog ⁻ + CO ₂	0	58	0	0	0	0	0	0	-58
39 Homog ⁻ + O ₂ → 4-MalAcAc ²⁻ + H ⁺	58	0	0	0	0	0	0	0	-58
40 4-FumAcAc ²⁻ → Fum ²⁻ + AcAc ⁻ + H ⁺	58	0	0	0	0	0	0	0	0
41 Pro → Δ ¹ -Pyr-5-Carb	0	0	0	0	0	0	52	0	0
42 Δ ¹ -Pyr-5-Carb → Glu ⁻ + H ⁺	98	0	0	0	98	0	0	0	0
Totals	910	1,076	-1,447	-1,879	-1,680	-16	652	72	-204
43 H ⁺ + HCO ₃ ⁻ → CO ₂ + H ₂ O	-910	910	-910						
Net balances	0	1,986	-2,357						
Equivalent O ₂ uptake					840	-8	326	18	204
Total O ₂ uptake							1,380		
H _{out} ⁺ equivalents					12	16	8	3	
H _{out} ⁺ by respiratory chain					20,160	-256	5,216	216	
Total H _{out} ⁺ by respiratory chain							25,336		

Conventions as in Table 2. Net charge of all metabolite input to mitochondria (except phosphates and bicarbonate) is +589, whereas that of all outputs produced in mitochondria is -1,768. Net decrease in charge of 2,357 provides a convenient check on proton plus bicarbonate balance. CarbP, carbamoyl phosphate; α-KBut, α-ketobutyrate; α-Am-β-Oxo-But, 2-amino-3-oxobutyrate; OH-Pyr, hydroxypyruvate; CysSulfin, cysteine sulfinate; Sulfinpyr, sulfinylpyruvate; Cyto c, cytochrome c; OH-Kyn, hydroxykynurenine; 3-OH-Anthr, 3-hydroxyanthranilate; α-Am-β-CarbMucSald, 2-amino-3-carboxymuconate-semialdehyde; α-Am-MucSald, 2-aminomuconate-semialdehyde; α-Am-Muc, 2-aminomuconate; α-KAdip, α-keto adipate; Sacchar, saccharopine; α-AmAdipSald, α-amino adipate-semialdehyde; α-AmAdip, α-amino adipate; GlutrylCoA, glutaryl-CoA; GlutnCoA, glutamyl-CoA; CrotCoA, crotonyl-CoA; β-OH-ButCoA, 3-hydroxybutyryl-CoA; IsoValCoA, isovaleryl-CoA; p-OH-Φ-Pyr, p-hydroxyphenylpyruvate; Homog, homogentisate; MalAcAc, malonyl acetoacetate; FumAcAc, fumarylacetoacetate; Δ¹-Pyr-5-Carb, 1-pyrroline-5-carboxylate. For other abbreviations see Tables 2, 5, and 12.

TABLE 14. Proton and charge movements associated with mitochondrial metabolite transport in liver

Translocation Process	Type	mmol/day			
		Protons		Positive charge	
		In	Out	In	Out
1 Asp _{out} ⁻ /Glu _{in} ⁻ · H _{in} ⁺	Antiport	796		796	
2 Glu _{out} ⁻ /H _{out} ⁺	Symport		403		
3 α-KG _{out} ²⁻ /Mal _{in} ²⁻ (363)	Antiport				
4 Mal _{out} ²⁻ /P _{i, in} ²⁻ (368)	Antiport				
5 P _{i, out} ⁻ /H _{out} ⁺	Symport*		282		
6 P _{i, in} ²⁻ → P _{i, in} ⁻ (368)	†				
7 2-PGA _{out} ²⁻ /(?)	(?)			172	
8 p-OH-Φ-Pyr _{in} ⁺ /H _{in} ⁺	Symport	58			
9 Orn _{in} ⁺ /Citr _{out} ⁺	Antiport			830	
10 Orn _{in} ⁺ /H _{out} ⁺	Antiport		46		
11 Pyr _{in} ⁻ /H _{in} ⁺	Symport	529			
12 α-KBut _{in} ⁺ /H _{in} ⁺	Symport	24			
13 Gln _{in} (18)	Neutral entry				
14 NH _{4, in} ⁺	‡			719	
15 Lys _{in} ⁺ /H _{out} ⁺	Antiport		76		
16 AcAc _{out} ⁺ /H _{out} ⁺	Symport		78		
17 Ser, Pro, Thr, Cys, Leu, Sarc, Kyn	Neutral entry?				
18 SO _{3, out} ²⁻ /(?)	(?)			72	
Totals		1,407	885	2,589	0
Net		522		2,589	

$$\text{ATP cost of translocation} = 522 \times \frac{1}{16} + 2,589 \times \frac{3}{16} \\ = 32\frac{5}{8} + 485\frac{7}{16} \approx 518$$

Movements of protons or positive charge into or out of liver mitochondria. Numbers in parentheses are millimoles per day of substances transported without obligatory proton or charge movements. ATP cost of metabolite transport estimated as in Table 3. Mechanism involved in translocation of some substances remains unclear, and in such cases no proton movements were invoked and ATP cost was calculated from the charge movement. For definitions of abbreviations see Tables 2, 12, and 13. * Conventions as in Table 6. † Conventions as in Table 6. ‡ Conventions as in Table 3.

acid-base balance in the hepatic mitochondrial matrix compartment. This form of "uncoupled respiration" must divert to reaction with cytoplasmic bicarbonate over 2.5 mol of matrix protons each day. As a result, 10% of the electron flow through the respiratory chain to oxygen that is associated with amino acid oxidation is uncoupled from ATP synthesis (Table 15).

The net effect of all of these events in the liver is the development of a net deficit of bicarbonate in the cytoplasm amounting to 640 mmol bicarbonate/day (Fig. 3).

D. Observations

Several further points about the metabolic process occurring in the liver are worthy of note.

1) The cytoplasmic generation and consumption of NADH are seen to be in perfect balance without the operation of any mitochondrial/cytoplasmic shuttles. Furthermore, only 1% of the mitochondrial malate production has to be translocated into the cytoplasm to achieve NADPH balance. The cellular location of each of the reactions producing or consuming reduced pyridine nucleotides appears to be strategically located so as to achieve this extraordinary balance.

2) Metabolic reactions that consume protons occur mainly in the cytoplasm, whereas those that consume bicarbonate occur exclusively in the mitochondrial matrix, the more alkaline compartment (see Tables 12 and

13). The net acid load of 640 mmol/day generated metabolically in the liver is neutralized by bicarbonate generated in the gut, kidney, and brain, as shown in Figure 3. In our example the overall effect of amino acid oxidation in the whole body is the consumption of 66 mmol HCO₃⁻/day (production of 66 mmol nonvolatile acid). Acid-base balance is maintained by two processes: first, the essentially obligatory oxidation to CO₂ and HCO₃⁻ of carboxylate anions presented in the diet and amounting to 50 mmol in our example, and second, the excretion of 16 mmol acid as titratable acidity utilizing the 16 mmol HPO₄²⁻ absorbed from the gut. In the steady state this acid excretion by the kidney cannot exceed the limit set by the intestinal uptake of HPO₄²⁻. Kidney function is continually adjusted such that the sum of the titratable acidity and metabolic generation of HCO₃⁻ from anion oxidation and ammoniogenesis brings the overall acid-base balance to zero.

3) Table 15 shows that the process of converting a physiological mixture of amino acids to glucose in the liver is in almost perfect energetic balance. The calculated net balance of 13 mmol ATP is only 0.2% of the 6,660 mmol ATP produced daily in the liver from amino acid oxidation. Perfect balance could be achieved readily by simply adjusting the amount of acetoacetate exported. This means that gluconeogenesis from a physiological mixture of amino acids is not normally limited by a need for ATP, as it might if it depended on ATP

TABLE 15. Calculation of the ATP balance in liver

	mmol/day	
Total H ⁺ _{out} respiratory chain (Table 13)	25,336	
H ⁺ _{out} by uncoupled respiration (Fig. 3)	-2,511	
Total H ⁺ _{out} available for oxidative phosphorylation	22,825	
Net mitochondrial ATP from amino acids*		1
Mitochondrial ATP made at substrate level (Table 13)		-1,879
Mitochondrial ATP made by oxidative phosphorylation		1,880
H _{in} ⁺ used to make mitochondrial ATP (×3)	5,640	
Remaining H _{in} ⁺ balance	17,185	
Cytoplasmic ATP by oxidative phosphorylation (÷4)		4,296
Cytoplasmic ATP at substrate level (Table 12)		-3,490
Cytoplasmic ATP used to transport positive charge (Table 14)†		-485
Cytoplasmic ATP used transport amino acids‡		-309
Net cytoplasmic ATP from amino acids		12
Net ATP balance of liver		13

* It was assumed that the consumption of ATP by reactions external to the amino acid oxidation process was 90% cytoplasmic and 10% mitochondrial. That is, of 13 mmol ATP made available to liver each day as a result of amino acid oxidation, 1 mmol was assumed to be utilized in mitochondrial matrix. † Only ATP cost of transporting positive charge is included because movement of protons has already been included in the adjustment for uncoupled respiration. ‡ Cost of amino acid transport was calculated on the assumption that all amino acids are taken into hepatocytes via a symport mechanism along with 1 Na⁺. Each Na⁺ was considered equivalent to 1/3 of a cytoplasmic ATP or ~4,000 cal/mol. Because the electrical potential across the hepatocyte sinusoidal membrane is ~40 mV, 1/4 of the energetic cost of pumping Na⁺ was attributed to the electrical term and 3/4 to the concentration gradient term. Thus when net cationic amino acid entry exceeds net anionic entry as it does in the liver, each extra positive charge entering the cell was considered equivalent to 1/2 ATP.

generated from some other substrate. Similarly, excess ATP generated as a by-product of the oxidation of amino acids does not accumulate in the liver and set a limitation on the maximal rate of the process.

VII. WHOLE BODY ENERGY BALANCE

We are now in a position to calculate the total ATP yield resulting from the oxidation of amino acids in humans (Table 16). After subtracting the ATP costs of endergonic reactions and of metabolite transport across membranes, there is a net yield of ~21.5 ATP for each amino acid processed on the average (shown in the 2nd column of Table 16 as 21,573 mmol ATP from 1,000 mmol amino acids). Of this amount roughly 7.5 ATP derive directly from amino acid oxidation; over one-half is produced in muscle, and much of the remainder is produced in the small intestine. An additional 13 ATP result when the glucose produced is oxidized, and one more ATP is gained from oxidation of the acetoacetate secreted by liver. The total net ATP yield amounts to 195 mmol ATP/g meat protein.

In Table 16 we summarize the total ATP production during amino acid oxidation and the portion of this ATP that is consumed as a part of the process of amino acid oxidation. These values are compared with those of the other major fuels in Table 17. Note that the common use of kilocalories of enthalpy to express the energetic value of foods introduces considerable error when comparing protein with either carbohydrate or fat. Some 23% more kilocalories are needed per net ATP produced from protein compared with carbohydrate.

VIII. METABOLIC PROCESSES

The enormous complexity of intermediary metabolism calls out for its subdivision into simpler compo-

nents that together constitute the whole. The usual approach has been division into pathways that typically focus on the flow of carbon from a given starting compound either to a particular end product or in some cases in a cyclic fashion back to the starting point. Most pathways produce in addition to the carbonaceous end product a series of by-products, such as reduced coenzymes and ATP, the further metabolism of which is usually not considered to be integral to the pathway. Rather these by-products are viewed as feeding into other pathways, such as the respiratory chain. Although this approach has proven its merit to biochemists for many decades, we emphasize the usefulness of an additional or supplementary approach that we believe has great utility for the molecular physiologist who wants to focus on the functional aspects of metabolism.

Rather than divide metabolism only into individual pathways, we suggest its division into larger units perceived as discrete metabolic processes. A metabolic process may be defined as an array of metabolic steps and pathways that collectively achieve a well-defined biochemical function while generating no by-products other than ATP (or ADP plus P_i) or substances released from the cells involved. Each metabolic process is thus a balanced process in which cofactors participating in catalytic amounts are neither produced nor consumed, except for ATP. When defined in this way metabolic processes become additive, i.e., the totality of metabolic events occurring in a cell or organ becomes the net sum of the several metabolic processes taking place, and no process interferes with any other by consuming or producing required cofactors, again except for ATP. The total net flux through any reaction step becomes the net of the fluxes associated with each process taking place. Some balanced metabolic processes require the joint

TABLE 16. Whole body ATP balance

Location	mmol/day				
	O ₂ consumed	ATP balance	ATP produced		ATP consumed
			Sub lev	Ox phos	
Liver					
Cytoplasmic metabolism	40	+806	0	4,296	3,490
Mitochondrial metabolism	1,380	+1	484	1,880	2,363
Charge transport*	0	-485			485
Amino acid uptake cost†	0	-309			309
Whole liver	1,420	+13	484	6,176	6,647
Gut					
Cytoplasmic metabolism	0	+2,302	531	2,125	354
Mitochondrial metabolism	397 ^{1/2}	+235	202	33	0
Charge transport*	0	-25			25
Amino acid uptake cost†	0	-184			184
Whole gut	397 ^{1/2}	+2,328	733	2,158	563
Muscle					
Cytoplasmic metabolism	0	+4,080	34	4,156	110
Mitochondrial metabolism	816	+446	230	390	174
Charge transport*	0	-6			6
Amino acid uptake cost†	0	-58			58
Whole muscle	816	+4,462	264	4,546	348
Kidney					
Cytoplasmic metabolism	0	+630	0	666	36
Mitochondrial metabolism	121 ^{1/2}	+66	54	12	0
Charge transport*	0	0			0
Amino acid uptake cost†	0	-27			27
Whole kidney	121 ^{1/2}	+669	54	678	63
Total from amino acids	2,755	+7,472	1,535	13,558	7,621
Oxidation of 351 glucose	2,106	+13,206	2,106	11,934	834
Oxidation of 39 acetoacetate	156	+895	78	858	41
Grand totals	5,017	+21,573	3,719	26,350	8,496

Values listed under ATP balance are net balance between production and consumption of ATP in each location. ATP produced by oxidative phosphorylation (Ox phos) is apportioned between cytoplasm and matrix as in Tables 4, 7, 10, and 15. Complete oxidation of glucose to CO₂ will produce 40 ATP. Cost of producing this ATP is 2 ATP for sugar phosphorylation and ³/₈ ATP to transfer the reducing power of 2 NADH from cytoplasm to matrix via malate and to transport 2 pyruvate into the matrix. Net yield of ATP from complete oxidation of glucose is thus 37 ⁵/₈ cytoplasmic ATP/mol. Acetoacetate oxidation will produce 24 ATP. Activation via succinyl CoA costs 1 ATP, and transport into mitochondria costs another ¹/₁₆ ATP, giving a net yield of 22 ¹⁵/₁₆ cytoplasmic ATP/mol. Total O₂ consumption can be conveniently checked for accuracy by reference to input data shown in Table 1. Overall oxidative process may be summarized as amino acids + O₂ + HCO₃⁻ → CO₂ + urea + creatinine + SO₄²⁻ + NH₄⁺ + H₂O. To write this as a balanced chemical reaction the composition and net charge of an average amino acid must be derived from the bottom line of Table 1. The overall process may then be expressed in chemical terms as: 1,000[(C_{4.850}H_{9.742}O_{2.458}N_{1.400}S_{0.036})^{+0.080}] + 5,017 O₂ + 66 HCO₃⁻ → 4,204 CO₂ + 664 CH₄ON₂ + 12 C₄H₇ON₃ + 36 SO₄²⁻ + 36 NH₄⁺ + 3,462 H₂O [where (C_{4.850}H_{9.742}O_{2.458}N_{1.400}S_{0.036})^{+0.080} is the average amino acid with a small positive charge, CH₄ON₂ is urea, and C₄H₇ON₃ is creatine]. Sub Lev, substrate level. * ATP cost listed here is for the transport of charged metabolites across the mitochondrial inner membrane. ATP cost of proton movements associated with this transport is already included in the order balances. † See Tables 4, 7, 10, and 15. Total overall cost of amino acid transport is only 2.6% of the energy obtained from amino acid oxidation.

participation of multiple cell types in several organs. When this occurs the components of the overall process taking place within each cell type must also be in balance for all substances except those that are exchanged between cells, excreted, or exhaled.

The reason for excepting ATP (or ADP and P_i) from the balance considerations is to allow flexibility in combining catabolic and anabolic processes to achieve the recognized functions of a particular organ. It is well known that a given energy-requiring anabolic process can be equally well supported by any of a variety of ATP-yielding catabolic processes. All that is necessary is that at any given moment the totality of the energy-yielding processes balance the totality of the energy-consuming events.

Examples of metabolic processes as we defined

them are oxidation of glucose to CO₂, conversion of glucose to triglycerides (lipogenesis), oxidation of triglycerides to CO₂ and glucose or to ketone bodies and glucose, and the very complex process considered here, oxidation of amino acids to CO₂ and glucose. It must be recognized that a metabolic process defined in this way cannot be rigidly defined in a quantitative sense. For example, depending on exactly what mixture of amino acids is consumed, the quantitative details of the metabolic process by which the amino acids are converted to glucose will vary. Moreover, the same metabolic process occurring in different species or even in different organs of the same species may also exhibit quantitative variations. These variations need not prevent us from recognizing and analyzing a core group of metabolic processes.

Our approach to metabolic processes has been in-

TABLE 17. Comparison of ATP yields of major fuels

Fuel	mol/mol					$\Delta H/\text{mol}$	$\Delta H/\text{ATP}_{\text{net}}$	$\Delta H/\text{liter O}_2$	$\Delta H/\text{g}$
	ATP produced			ATP consumed	Net ATP balance				
	Total	Sub lev	Ox phos						
Glucose	40	6	34	2.4	37.6	-672.15	-17.9	-5.00	-4.05*
Tripalmitin†	420	27	393	8.4	411.6	-7,590	-18.4	-4.67	-9.42
Meat protein (per amino acid)	30.1	3.7	26.4	8.6	21.5	-475	-22.1	-4.23	-4.32

All ATP calculations are based on the assumption that 90% of the net ATP yielded is utilized in cytoplasm or nucleus and 10% in mitochondrial matrix. Sub Lev, substrate level; Ox phos, oxidative phosphorylation; ΔH , change in enthalpy. * The value is 3.73 kcal/g glucose, 4.15 kcal/g (dry) glycogen, and 4.05 kcal/g dietary carbohydrate assumed to be 60% starch and 40% sucrose. † In calculating ATP yields for tripalmitin, it was assumed that the glycerol moiety will be converted to glucose by liver and then oxidized to CO_2 in the periphery. ΔH for tripalmitin oxidation was calculated from heats of formation of palmitic acid, glycerol, and water and the esterification heat found for converting myristic acid to trimyristin. Heat values are from Appendix Table 1 in Ref. 10a, except for the protein value, which is the old value of Loewy (44a).

spired by and built on the work of Flatt and Ball (27), who analyzed the metabolic process of lipogenesis from glucose in rat adipose tissue. Their analysis was central in advancing our knowledge of the regulation of lipogenesis by hormones and in understanding the factors that set the maximal rates of lipogenesis. A major achievement was the recognition that the maximal rate was limited not by the enzymatic capacity of any step directly intervening between glucose and palmitate but by the capacity of the tissue to utilize the ATP produced as a by-product of lipogenesis from glucose (26). A similar conclusion applies to gluconeogenesis from glutamine in the kidney (31).

IX. LIVER OXIDATION OF AMINO ACIDS

As conceived here, the major metabolic process involved in the metabolism of dietary amino acids is their oxidation to glucose and CO_2 . The major alternative would be a process in which the amino acid carbon is diverted to triglycerides rather than to glucose. This is likely to occur mainly when large quantities of carbohydrate are consumed for extensive periods along with the amino acids (2) and is not considered further here. The commonly held view that excess dietary amino acids are simply totally oxidized to CO_2 by the liver lacks experimental support and is untenable because of ATP balance considerations. Complete oxidation to CO_2 by the liver of the quantity of amino acids present in a typical diet (15% of the total calories) would produce far more ATP than the liver could utilize.

The simplest way to make this point clear is to examine the oxygen consumption data. The liver consumes $\sim 50 \text{ ml O}_2/\text{min}$ or $\sim 3,000 \text{ mmol/day}$ (28). As shown in Table 16, nearly one-half of this oxygen (1,420 mmol) is consumed just in the process of converting the daily supply of amino acids to glucose and small amounts of acetoacetate. The remaining daily oxygen consumption of the liver (1,580 mmol) is less than that needed to completely oxidize to CO_2 the glucose and acetoacetate produced from the amino acids (2,262 mmol; Table 16).

Therefore, even if no other substrate were consumed by the liver, i.e., no dietary carbohydrate or fat or alcohol was burned, it would not be possible for the liver to oxidize its daily supply of amino acids completely to CO_2 and water. Given the certainty that many other substances are in fact oxidized by liver, we conclude that the major pathway of amino acid metabolism in liver is their oxidative conversion to glucose.

This means that gluconeogenesis should not be viewed as a process occurring only or even primarily during fasting. Most in fact occurs prandially while amino acids are being absorbed and processed. On days when $\geq 110 \text{ g}$ protein are consumed, gluconeogenesis from amino acids must extend throughout at least 12 of 24 h to not exceed the oxygen uptake rate limitation and probably extends over most of each such 24-h period.

The likely biochemical explanation for the liver not oxidizing amino acids to CO_2 is twofold. 1) Pyruvate dehydrogenase is probably severely inhibited during amino acid oxidation because of high levels of ATP, NADH, and acetyl-CoA present in liver mitochondria. As a result, entry of pyruvate carbon into the tricarboxylic acid cycle is minimal. 2) Pyruvate kinase activity is low because of low levels of cytoplasmic ADP and fructose 1,6-diphosphate and high levels of alanine. In essence the gut forces the liver into its gluconeogenic mode by secreting large amounts of alanine into the portal vein whenever protein is consumed. Consequently, most amino acid carbon, as well as dietary carbohydrate, is channeled to glucose or glycogen.

In our oxygen consumption calculations we did not make an adjustment for the fact that $\sim 10\%$ of parenchymal hepatocytes, the extreme perivenous cells, do not possess the capacity to oxidize amino acids and generate urea and thus must subsist on other fuels such as alcohol and glucose (34). These perivenous cells scavenge ammonium by synthesizing glutamine from any ammonium not converted to urea by the upstream periportal cells, a process of great importance in maintaining a low plasma ammonium level and in adjusting to major acidotic challenges (32). At normal plasma pH, roughly equal quantities of glutamine are produced by

perivenous cells and consumed by periportal cells. Thus this intercellular cycling of glutamine normally approximately cancels out when considering the net metabolism of the liver as a whole, its only effect being to increase oxygen consumption by $\sim 2\%$, and we have ignored it in our calculations.

The biochemical advantages of oxidizing most amino acids in the liver via glucose are obvious. Only the liver need expend the energy needed to synthesize the entire complex array of enzymes involved in amino acid oxidation. Note that nearly one-half of the input amino acid carbon is converted to either glucose or acetoacetate (2,262 of 4,850 mmol carbon). Thus virtually all organs of the body can utilize indirectly some two-thirds of the energy available from protein fuels (Table 16) and yet be spared the task of synthesizing amino acid catabolic enzymes. Moreover, this allows animals to tolerate a diet quite high in protein without the risk of oversupplying the liver and starving the periphery, as might occur if amino acids were completely catabolized to CO_2 in the liver.

In this regard we emphasize the advantage of oxidizing some of the amino acids in the periphery. When animals consume diets very high in protein, the oxidative processing of the amino acids by the liver would be restricted if there were a large net ATP yield in the process: more ATP cannot be synthesized than the liver utilizes each day. In our example, if the BCAA were oxidized in the liver, another 816 mmol O_2 would be required (Table 16). This represents one-half of the remaining 1.6 mol O_2 (see sect. IX) available for oxidative processes in the liver and would mean that very little besides amino acids could be oxidized by the liver. In our example protein made up only 15% of the total caloric intake; if diets substantially higher in protein are to be tolerated, some amino acids must be oxidized in the periphery. Because the BCAA yield large amounts of ATP relative to their yield of glucose, they are a good choice for this purpose. We suggest that this is the fundamental reason BCAA are frequently oxidized in muscle in higher animals. It is conceivable that the oxidation of other amino acids may also be shifted to peripheral organs on diets unusually high in protein, but we know of no data bearing on this question.

We note in this connection that the diet of humans has changed substantially in the last few thousand years while our genes remain virtually the same as in the paleolithic era. Estimates of the dietary composition of paleolithic humans suggest that proteins supplied roughly one-third of the calories (18), the difference being made up by a lesser fat content. Such a diet would require that virtually the entirety of the oxygen consumption of the liver be utilized to process amino acids to glucose and could be tolerated only if the BCAA were processed outside the liver.

Our calculations indicate a production of 3.22 g glucose/g urinary nitrogen. This number is somewhat lower than the value of 3.66 obtained by Schulz (55) and by McGilvery (47), whose calculations did not take into account the contribution of organs other than the liver.

Both numbers are consistent with the glucose-to-nitrogen ratio observed many years ago in the urine of dogs fed lean meat when their capacity to utilize glucose or to reabsorb glucose from the proximal renal tubules was inhibited with phlorizin (59).

We did not include in our calculations the concomitant gluconeogenesis arising from lactate undergoing the Cori cycle or from glycerol liberated during triglyceride oxidation. These are distinct metabolic processes that must be added to amino acid oxidation to obtain a more complete picture of daily liver metabolism.

X. INTESTINAL OXIDATION OF AMINO ACIDS

It was observed by Windmueller and Spaeth (68) that $\sim 80\%$ of the total CO_2 produced by the small intestine of rats derived from the oxidation of the three amino acids: glutamine, glutamate, and aspartate. Our calculations suggest that a similar fraction of the total oxygen uptake of the human jejunum results from the oxidation of these amino acids. We did not find any direct measurements of the oxygen consumption of the human jejunum either in vivo or in vitro. We attempted to estimate this value as follows. Together, the human liver and alimentary tract consume 75 ml O_2 /min (37). Because the liver consumes 47 ml, this leaves 28 ml/min for the total gastrointestinal tract or 1,800 mmol/day. By weight, the small intestine is 57% of the total gastrointestinal tract and the jejunum is 40% of the small intestine (15). If one corrects for the greater oxygen consumption per unit weight of the jejunum than the ileum (65) and of the small intestine than the colon and stomach (17), the total oxygen consumption of the human jejunum may be expected to fall in the range of 450–550 mmol/day. Taking 500 mmol/day as the best estimate, our calculated value of 400 mmol/day (Table 2) as arising from the three amino acids would be 80% of the total. Unless the human jejunum differs greatly in its metabolism of amino acids from the other mammalian intestines that have been studied, it seems very likely that the major fuels of the jejunum are glutamine (both luminal and arterial) and glutamate and aspartate (luminal only). In contrast, skeletal muscle in a normally active male may be expected to consume $\sim 12,000$ mmol O_2 /day of which only 7% comes from amino acids (see Table 5), whereas the kidneys consume $\sim 1,000$ mmol O_2 with only one-eighth attributable to amino acid metabolism (see Table 8). Thus for only two organs, jejunum and liver, will amino acids be the quantitatively dominant fuels.

XI. CHOLESTEROGENESIS

As shown in Figure 6, conversion of aromatic amino acids and of leucine to mitochondrial acetoacetate amounts to 78 mmol/day in our example. The metabolic fate of this ketone body is unclear; it may well be released from the liver along with glucose for oxidation in

the periphery. In our calculations we wanted to minimize our maximum error and so assumed that one-half of the acetoacetate was released and one-half was activated to acetoacetyl-CoA by the cytoplasmic synthetase first demonstrated by Stern (58). If human liver has the same acetoacetate-CoA synthetase content as rat liver (8), if this synthetase has the same Michaelis constant (K_m) for acetoacetate as in rats, and if the acetoacetate level in human liver is 20 μ M as in fed rats, human livers would convert ~ 50 mmol acetoacetate to acetoacetyl-CoA per day. Of the acetoacetyl-CoA formed in rat liver cytoplasm, 75% is converted to acetyl-CoA and 25% to cholesterol (8). Therefore 12 mmol acetoacetyl-CoA may well be converted to 2 mmol cholesterol daily in human liver. This would amount to ~ 770 mg cholesterol/day, a large fraction of the total daily *de novo* cholesterologenesis in humans. For simplicity we did not include cholesterologenesis in our diagrams or calculations.

XII. METABOLIC PATHWAYS IN LIVER

We emphasize the close linkage between flux through the urea cycle and flux from amino acid carbon to glucose. In fact the two pathways share the common step wherein aspartate is converted to fumarate while citrulline is converted to arginine. This assures that urea formation will go hand in hand with glucose formation and nitrogenous intermediates will not accumulate. It means in effect that argininosuccinate synthetase and lyase should be considered *de facto* enzymes on the main gluconeogenic pathway in the liver. This circumstance has often been overlooked when considering rate control of gluconeogenesis in the region between pyruvate and PEP. Rate-control studies with perfused liver or isolated hepatocytes have often been conducted with unphysiological mixtures of gluconeogenic precursors. The flexibility of liver metabolism is such that alternate pathways of gluconeogenesis may have resulted that would rarely be used *in vivo*. Because cross-over studies (51) clearly indicate an important site of rate control lies between pyruvate and PEP, we feel it is important to initiate studies that are physiologically realistic to explore the possible role of regulation of urea cycle enzymes in the control of gluconeogenesis.

Although there is no known transport mechanism by which oxaloacetate may directly cross the inner membrane of the mitochondria, there are four metabolic pathways by which oxaloacetate formed in liver mitochondria during gluconeogenesis may be converted to cytoplasmic oxaloacetate. The relative flow through each of these pathways is fixed by balance considerations, although two of the pathways seem somewhat more flexible in adjusting to metabolic circumstances. Consider first the main stream pathway in which oxaloacetate exits the mitochondria after transamination to aspartate with the cytoplasmic aspartate reaching oxaloacetate via fumarate and malate (Fig. 6, heavy arrows). Flow through this pathway is clearly fixed by the extent of the concomitant ureagenesis, i.e., by nitro-

gen balance considerations, and thus this flow is not independently variable. It is the dominant pathway during gluconeogenesis from a mixture of amino acids under most circumstances.

In the second pathway oxaloacetate also exits the mitochondria after transamination to aspartate, but the aspartate is again simply transaminated to oxaloacetate in the cytoplasm. In contrast to the first pathway, no cytoplasmic NADH is formed along with the cytoplasmic oxaloacetate. If this oxaloacetate is to reach glucose an alternative source of cytoplasmic NADH must be found. Flow through this pathway is therefore dependent on the NADH balance of the cytoplasm. In our example this flow could be estimated as the supply of lactate less the amount of hydroxypyruvate formed from serine (see Fig. 6 and APPENDIX A). In our example only 28 mmol oxaloacetate take this route, although if normal total daily inputs of lactate and glycerol were included in our calculations this flux would increase by ~ 200 –400 mmol. Futile recycling of newly formed PEP back through pyruvate kinase to pyruvate would also be expected to increase flow through this pathway.

In the third possible pathway, mitochondrial oxaloacetate is reduced to malate, which exits to the cytoplasm to be reoxidized to oxaloacetate via malate dehydrogenase. Flow through this pathway is rather flexible (see next section). It does not exceed 5 mmol in our example, although it would occur to a greater extent when protein breakdown occurs during fasting. This is because a greater fraction of the glutamate and aspartate derived from muscle or liver proteolysis is metabolized in the liver and less in the gut compared with dietary protein. When these amino acids are converted to glucose in the liver, a supplementary source of cytoplasmic NADH is required, and this third pathway is the most probable source. The relative supplies of aspartate and NH_4^+ as sources of urea nitrogen also influence this pathway (see next section). Flow through this third pathway should not be confused with the flow through the pyruvate-malate cycle needed to balance cytoplasmic NADPH (70 mmol in our example), which shares some of the same steps.

The fourth possible pathway by which mitochondrial oxaloacetate could reach cytoplasmic oxaloacetate involves its decarboxylation to PEP within the mitochondrial matrix. The PEP would exit to the cytoplasm via an antiport and join the main flow at the level of cytoplasmic PEP. In this case it would be the cytoplasmic/mitochondrial balance of HCO_3^- that would be affected, since there is a net transfer of mitochondrial matrix protons to the cytoplasm by this pathway. This pathway appears to be very flexible; indeed many species do not synthesize the mitochondrial PEP carboxykinase needed for its operation. In our example this flow could not exceed 5 mmol/day, which is far too small to significantly alleviate the acid-base balance problem of the mitochondrial matrix. For this reason we chose to ignore this pathway and omit it from the diagrams. We know of no quantitative data on the extent of flow through this pathway under physiological conditions,

nor can we conceive of a method to make such measurements.

XIII. ROLE OF UREASE

In the scheme shown in Figure 6 we assume that urease in the colon lumen generates 400 mmol ammonium ions/day by cleavage of 200 mmol urea. In fact there is likely to be considerable variability in this number. The overall effect of reducing gut urease activity from 200 to 100 mmol/day would be rather small. Total urea synthesis would drop from 864 to 764 mmol, reducing the amount of carbamoyl phosphate required by 100 mmol. Because the supply of ammonium ions from the colon lumen would be reduced by 200 mmol, formation of NH_4^+ from mitochondrial glutamate dehydrogenase would have to increase by 100, from 61 to 161 mmol/day. Mitochondrial α -ketoglutarate balance would be maintained by decreasing glutamate transamination by 100 mmol. There would thus be 100 mmol fewer of aspartate leaving the mitochondria, 696 rather than 796 mmol, in exchange for glutamate, and this would be balanced by reducing glutamate exit from 403 to 303 mmol/day. The flexibility of the third pathway for conversion of mitochondrial oxaloacetate to cytoplasmic oxaloacetate is illustrated by the fact that the flow of malate into the cytoplasm would now increase from 5 to 105 mmol, thereby maintaining constant the flow of carbon to glucose and the supply of cytoplasmic NADH. Overall there would be an increase in the net ATP balance of 539 mmol or ~ 5.4 for each urea spared cleavage. This number is greater than the apparent ATP cost per urea synthesized of 4.0 (2 for argininosuccinate synthesis and 2 for carbamoyl phosphate synthesis) because of two factors. Lessened transport across the mitochondrial membrane of aspartate, ornithine, and NH_4^+ spares 0.75 ATP for each urea spared cleavage. In addition fewer HCO_3^- are removed from the mitochondrial matrix by metabolic reactions and transport steps so that less uncoupled respiration is required to maintain acid-base balance. This saves 0.64 ATP for each urea spared cleavage. In general, reducing gut urease activity even to zero could be readily tolerated as could increasing it well beyond the 200 mmol/day assumed here.

XIV. COMPARTING OF UREA CYCLE

One of the most remarkable features of the urea cycle is its division between the cytoplasmic and mitochondrial compartments of the cell. The significance of this division is gradually becoming clearer. Consider, for example, the fact that bicarbonate fixation into urea occurs within the mitochondrial matrix. We pointed out in Tables 12–14 and Figure 3 that it is only in the cytoplasmic compartment of liver that a net production of bicarbonate occurs during amino acid oxidation. There is a net consumption of bicarbonate from the matrix compartment of $>1,200$ mmol/day quite apart from the

action of carbamoyl phosphate synthetase. The advantage of having carbamoyl phosphate synthetase located in the mitochondrial matrix arises from two factors. First, in the matrix it utilizes “cheap ATP,” i.e., ATP synthesized at a cost of only three protons per high-energy bond rather than four protons for cytoplasmic ATP. This reduces the energetic cost of urea synthesis by ~ 0.5 ATP/mol. The second factor is more subtly related to the translocation of protons by the respiratory chain. From the daily oxygen consumption of the liver this flux of protons can be estimated to be 65,000 mmol/day, virtually all of which simply recycle with the formation of 15,000 mmol ATP. These fluxes dwarf the bicarbonate fluxes associated with amino acid oxidation, which amount to a production of $\sim 2,200$ mmol in the cytoplasm and a matrix consumption of $\sim 2,900$ mmol (see Fig. 3). The pH gradient established by the respiratory chain therefore is not appreciably disturbed by amino acid oxidation, remaining ~ 0.8 pH unit, matrix alkaline (3, 60). Thus the reactions producing or consuming bicarbonate during the oxidation of amino acids are seen to be distributed between the cytoplasm and mitochondria in such a way as to be facilitated at the cost of energy made available by the respiratory chain. Reactions consuming bicarbonate occur largely in the matrix where bicarbonate is abundant; those producing bicarbonate tend to occur in the cytoplasm where bicarbonate levels are lower.

The advantage of positioning the site of ammonium removal within the mitochondrial matrix is not so clear. It is well established that the true substrate for carbamoyl phosphate synthesis is NH_3 rather than NH_4^+ (13). If NH_3 freely permeates the inner mitochondrial membrane, it should be nearly equal in concentration in both cell compartments. However, if permeation is partial, the matrix location would be favored if transport into the matrix were to occur in the form of the NH_4^+ cation because of the electrical potential across the inner mitochondrial membrane. This would lead to an active accumulation of ammonium within the mitochondria. We would point out that the K_m of purified carbamoyl phosphate synthetase for NH_3 is near $40 \mu\text{M}$ (13); when measured with intact mitochondria the half-maximal constant ($K_{1/2}$) for the process is $\sim 15 \mu\text{M}$ (13), and when measured with hepatocytes or in vivo the $K_{1/2}$ of ureagenesis for NH_3 is $2\text{--}7 \mu\text{M}$ (12). Thus it is possible that plasma levels of $4 \mu\text{M}$ NH_3 produce $40 \mu\text{M}$ levels within the matrix.

It is clear that not all biological membranes are freely permeable to NH_3 . For example, some membranes of the renal tubules must not have this property (14, 29, 38). We note that uricotelic animals also fix NH_3 from the mitochondrial compartment. In this case glutamine synthetase is located intramitochondrially (63), and the glutamine formed then exits the mitochondria to participate in purine synthesis in the cytoplasm. Furthermore, the induction of transport systems for NH_4^+ in bacteria grown with low concentrations of ammonium as the nitrogen source (39) clearly indicates the potential for such a process in mitochondria. For these sev-

eral reasons we suggest that the mechanism of NH_4^+ transport into mitochondria be carefully reinvestigated.

XV. MITOCHONDRIAL ACID-BASE BALANCE

An important aspect of the acid-base balance considerations associated with amino acid oxidation remains to be considered. When fatty acids are oxidized, the mitochondrial compartment of the cell experiences no net acid or base load. This is because fatty acids enter these organelles in an uncharged form either as undissociated acids or as their carnitine esters, and the products that leave the mitochondria, CO_2 and water, are also uncharged. However, in the case of amino acid oxidation the net charge of the complex array of metabolites entering the liver mitochondria differs from that of the products generated that leave the mitochondria. As a result a nonvolatile acid load develops within these organelles that is very substantial. In fact, it exceeds the net fixed-acid load amino acid oxidation places on the whole body (here estimated at 66 mmol/day) by more than an order of magnitude.

Liver mitochondria apparently maintain their acid-base balance during amino acid oxidation in two ways: they secrete protonated phosphates to the cytoplasm, and they secrete protons via the respiratory chain proton pump in a form of "uncoupled respiration." Only a small part of the acid load appears to be accommodated with phosphates. As shown in Table 14, 368 mmol phosphate enter the mitochondria in the form of HPO_4^{2-} on the dicarboxylate carrier. Within the matrix this phosphate accepts protons to form H_2PO_4^- , which apparently is the form exported on the P_i symport (41). We assume that the 86 mmol of 2-phosphoglycerate also leave the mitochondria as the species with a single negative charge on the phosphate moiety. Thus 368 mmol acid are effectively transferred from the matrix to the cytoplasm by these movements of phosphate.

This leaves an enormous bicarbonate deficit within the liver mitochondrial matrix estimated at 2,511 mmol/day (see Fig. 3). The only way known to us by which a deficit of this magnitude can be balanced is through the operation of the respiratory chain proton pump. We conclude that approximately this quantity of protons must be pumped from the matrix to the cytoplasm via the respiratory chain. If acid-base balance is to be accomplished, these protons cannot be allowed to reenter the matrix with the formation of ATP as in the normal process of chemiosmotic oxidative phosphorylation. Thus the oxygen consumption associated with the movement of these protons must in effect constitute uncoupled respiration. It should be regarded as a normal physiological process essential for acid-base balance within the mitochondrial matrix during amino acid oxidation. It differs from conventional uncoupled respiration in not being dependent on the leakage of protons back into the matrix through the inner mitochondrial membrane.

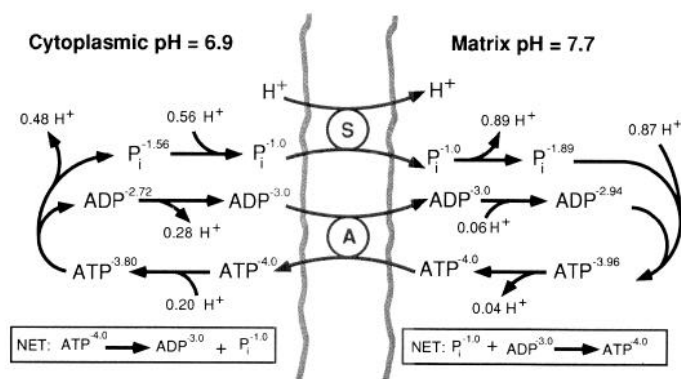


FIG. 7. Movement of adenylates and P_i across inner mitochondrial membrane. Shown are proton dissociations required when species of ATP, ADP, and P_i that cross the membrane bear exact charges shown, at cytoplasmic and matrix pHs measured in hepatocytes by Strzelecki et al. (60). It was assumed that the dissociation constant of ATP is 6.3, of ADP is 6.5, and of P_i is 6.8. Adenylates were assumed to cross via antiport (A), which is specific for unchelated species shown (40), whereas P_i crosses with a proton via symport (S).

When the methodology developed here for analyzing amino acid oxidation is applied to glucose oxidation, an interesting point emerges that has apparently not been widely recognized previously. Here too a bicarbonate deficit arises in the mitochondrial matrix. Although the deficit amounts to only 2 mol/mol glucose oxidized to CO_2 and water, because ~ 2 mol sugar are oxidized each day, the total deficit of 4 mol/day is even greater than the mitochondrial matrix acid load arising from amino acid oxidation. In this case the bicarbonate deficit does not arise from mitochondrial reactions; pyruvate enters the matrix on a symport with a proton and thus in an uncharged form. However, the NADH generated in the cytoplasm as glucose is oxidized to pyruvate must be reoxidized, and if this is accomplished via the "Borst cycle" involving oxaloacetate, malate, α -ketoglutarate, and glutamate, one proton will pass into the matrix for each NADH oxidized. We took this factor into account in calculating the net ATP yield from glucose as $37^{5/8}$ (Table 17).

For the purpose of avoiding any possible confusion, we emphasize that the cyclic series of reactions by which ATP is formed in the mitochondrial matrix by oxidative phosphorylation and later consumed in the cytoplasm does not alter the acid-base balance of either compartment. This point is most easily discussed by reference to Figure 7, which shows the movement of adenylates and P_i across the mitochondrial inner membrane during cellular metabolism. At the pH of the matrix, here assumed to be 7.7 (3, 5, 60), it might appear that the formation of ATP from ADP and P_i leads to a net uptake of protons that would be released subsequently in the cytoplasm when the ATP is reconverted to ADP and P_i . However, closer inspection of Figure 7 reveals that the protons picked up during ATP synthesis in the matrix are exactly balanced by those released from ADP and P_i when they reenter the matrix. Thus no net translocation of protons across the inner membrane of the mitochon-

dria occurs during these events. Note that neither the exact pH of either compartment nor the particular ionic species of adenylates or P_i translocated by the carriers is material to this argument. The proton entering the matrix with P_i balances the extra proton recycled from the matrix back to the cytoplasm by the respiratory chain when ATP is utilized in the cytoplasm and thus also does not enter into acid-base balance considerations.

XVI. WHOLE BODY ACID-BASE BALANCE

Recently Atkinson and Bourke (4) argued that the acid-base threat associated with amino acid oxidation is not acidosis as traditionally viewed but alkalosis. They base their view on the notion that amino acid oxidation proceeds in two phases. In the first, amino acids are converted to neutral products plus ammonium and bicarbonate ions; in the second, ammonium and bicarbonate are assembled into urea for disposal. According to this view, were it not for ureagenesis, huge quantities (1,342 mmol/day in our example; see Table 1) of bicarbonate would accumulate and cause metabolic alkalosis. Thus it is only by synthesizing urea that the liver is able to protect the body from alkalosis. The ammonium ions produced concurrently do not disturb acid-base balance because the nitrogen atoms involved were already protonated when present as amino groups, and thus no uptake or release of protons occurs during their formation, with but a few exceptions. Conversion of amino acid carboxylate groups to CO_2 does, of course, represent the metabolic destruction of fixed nonvolatile acid. It results in the uptake of protons and the generation of bicarbonate and thus leads to alkalosis. Atkinson and Bourke (4) suggest further that ureagenesis is driven by the need to dispose of this bicarbonate rather than by the need to dispose of nitrogen. When ureagenesis has eliminated all the excess bicarbonate produced, urea synthesis stops and any extra ammonium is converted to glutamine and eliminated in the urine as ammonium.

We salute Atkinson and Bourke for bringing a creative and stimulating fresh analysis into the acid-base balance field, even though we cannot agree with all of their views. An examination of Figure 6 reveals that amino acid oxidation cannot be simply divided into the two phases proposed by Atkinson and Bourke. To do so would be entirely artificial and without regard for the reality of the process. For example, much of the nitrogen that appears in urea need not pass through the ammonium pool at all. Bicarbonate is generated at many points throughout the process, as listed in Tables 12 and 13. A large share of the bicarbonate production occurs in liver cytoplasm in the final stages of the process as carbon flows from oxaloacetate to triose phosphate and not in the early stages when amino acid carbon is fed into the main stream of carbon flow. Therefore there is in fact no intermediate stage at which there is a true threat from alkalosis in the liver, as suggested by Atkinson and Bourke. Certainly this is not the case at the

site of bicarbonate uptake during ureagenesis, the mitochondrial matrix. This compartment experiences a net consumption of bicarbonate throughout the process, and it is only the continued functioning of the respiratory chain that protects this compartment from severe acidosis.

On balance, whole body amino acid oxidation generates nonvolatile acids, 66 mmol/day in our example. To maintain acid-base balance during this process the kidney increases its excretion of titratable acidity, 16 mmol/day in our example. Were there no other alkalizing metabolic processes occurring, this excretion would have to increase to 66 mmol to maintain acid-base balance. We have assumed that the diet contains 50 mmol of anions such as malate and citrate whose oxidation to CO_2 adds 50 mmol to the whole body bicarbonate pool and maintains the balance. Thus we hold to the traditional view that amino acid oxidation presents the body with an acidotic threat, although we do agree with Atkinson and Bourke when they point out the importance of the liver in maintaining whole body acid-base balance. We have defended elsewhere (12) our view that under physiological conditions the rate of ureagenesis is determined primarily by the amount of nitrogen that must be excreted and in particular by the NH_3 concentration of the plasma. Neither plasma pH nor bicarbonate per se appeared to be a major determining factor under our experimental conditions.

XVII. SUMMARY

Significant gaps remain in our knowledge of the pathways of amino acid catabolism in humans. Further quantitative data describing amino acid metabolism in the kidney are especially needed as are further details concerning the pathways utilized for certain amino acids in liver. Sufficient data do exist to allow a broad picture of the overall process of amino acid oxidation to be developed along with approximate quantitative assessments of the role played by liver, muscle, kidney, and small intestine.

Our analysis indicates that amino acids are the major fuel of liver, i.e., their oxidative conversion to glucose accounts for about one-half of the daily oxygen consumption of the liver, and no other fuel contributes nearly so importantly. The daily supply of amino acids provided in the diet cannot be totally oxidized to CO_2 in the liver because such a process would provide far more ATP than the liver could utilize. Instead, most amino acids are oxidatively converted to glucose. This results in an overall ATP production during amino acid oxidation very nearly equal to the ATP required to convert amino acid carbon to glucose. Thus gluconeogenesis occurs without either a need for ATP from other fuels or an excessive ATP production that could limit the maximal rate of the process. The net effect of the oxidation of amino acids to glucose in the liver is to make nearly two-thirds of the total energy available from the oxida-

tion of amino acids accessible to peripheral tissues, without necessitating that peripheral tissues synthesize the complex array of enzymes needed to support direct amino acid oxidation.

As a balanced mixture of amino acids is oxidized in the liver, nearly all carbon from glucogenic amino acids flows into the mitochondrial aspartate pool and is actively transported out of the mitochondria via the aspartate-glutamate antiport linked to proton entry. In the cytoplasm the aspartate is converted to fumarate utilizing urea cycle enzymes; the fumarate flows via oxaloacetate to PEP and on to glucose. Thus carbon flow through the urea cycle is normally interlinked with gluconeogenic carbon flow because these metabolic pathways share a common step.

Liver mitochondria experience a severe nonvolatile acid load during amino acid oxidation. It is suggested that this acid load is alleviated mainly by the respiratory chain proton pump in a form of uncoupled respiration. Whole body acid-base balance is maintained dur-

ing amino acid oxidation by the metabolic generation of bicarbonate in the kidneys, in the mucosa of the small intestine, and in other peripheral tissues at rates nearly equal to the rate of fixed acid production by the liver; the small excess of fixed acid is compensated by urinary titratable acidity.

APPENDIX A

The following procedure is recommended for calculating the net flow through each of the reaction steps involved in the oxidation of amino acids in the liver.

1) Begin by filling in those net fluxes that follow directly from the amino acid inputs, e.g., the total supply of acetyl-CoA, sarcosine, and methylmalonyl-CoA.

2) Obtain the amount of pyruvate entering the mitochondria by adding to the inputs from alanine, serine, and lactate the amount coming from the malate cycle (M). The malate cycle is estimated by assuming it to be the only source of cytoplasmic NADPH and hence is readily obtained by equating it to the cytoplasmic consumption of NADPH

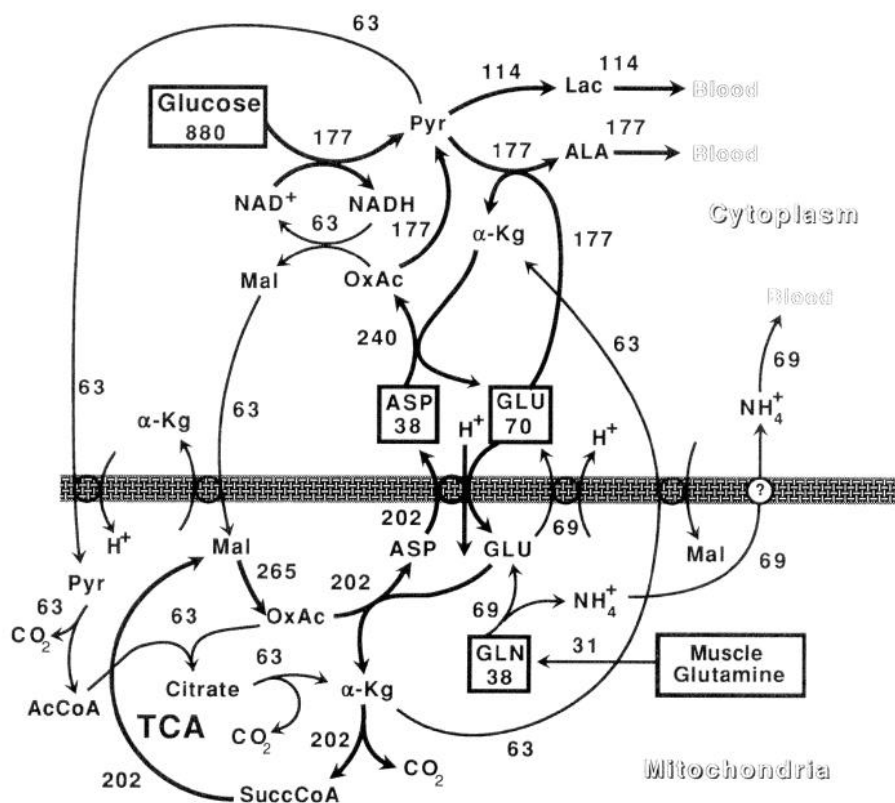


FIG. 8. Details of metabolic process occurring in intestinal mucosal cells during oxidation of daily supply of amino acids in humans. Thick bar across center represents inner membrane of mitochondria, with cytoplasmic events shown above and matrix events shown below. Circles in membrane indicate recognized symports and antiports, except in case of ammonium ions whose mechanism of transport is unknown; α -ketoglutarate-malate (Mal) antiport is drawn twice for convenience. Dietary glutamine input was set equal to two-thirds of dietary content based on observations in rats of Windmueller and Spaeth (68) ($56 \times \frac{2}{3} = 37.33$, rounded to 38). Glutamine input from arterial supply was set equal to output from muscle (i.e., 76; see Fig. 9 in APPENDIX B) minus amount consumed by kidney (i.e., 45; see Fig. 10 in APPENDIX B), since net hepatic utilization of glutamine is minor when plasma pH is normal. Only other value needed to determine rate of each reaction shown is rate of lactate production, which was calculated from total carbon balance. Windmueller and Spaeth (66, 67) showed that 60% of input amino acid carbon, whether aspartate, glutamate, or glutamine, was converted to $\text{CO}_2 + \text{HCO}_3^-$ in rat small intestine; hence lactate carbon was set equal to 40% of input amino acid carbon, which rounds to 114 mmol/day. Cytoplasmic NADH balance then requires that flow from cytoplasmic oxaloacetate to malate be $177 - 114 = 63$, which is also amount of pyruvate oxidized via tricarboxylic acid cycle (TCA). With these values, all others are readily calculated. For definitions of abbreviations see Fig. 1.

FIG. 9. Details of metabolic process occurring in skeletal muscle during oxidation of daily supply of amino acids in humans. Irregular double line across center represents inner membrane of mitochondria. Arrows with open arrowheads trace flow of amino acid carbon to glutamine. Double-headed arrows designate reactions utilized for dual purposes. Calculation of metabolic flows requires, in addition to amino acid input information, only data on ratio of glutamine to alanine released. Elia and Livesey (19) showed that $\frac{7}{8}$ of nitrogen released from muscle in humans was glutamine. We rounded this value to 76 mmol/day. Note that flow from mitochondrial oxaloacetate to aspartate must equal sum of isoleucine and valine inputs minus flow to glutamine, i.e., $(56 + 54) - 76 = 34$. With these values, all other flows are readily obtained. AcAc, acetoacetate; AcAcCoA, acetoacetyl-CoA; BCAA, branched-chain amino acids; BCKA, branched-chain α -keto acids; Mal, malate; MeButCoA, 2-methyl butyryl-CoA; ProCoA, propionyl-CoA; Succ, succinate. For definitions of other abbreviations see Fig. 1.

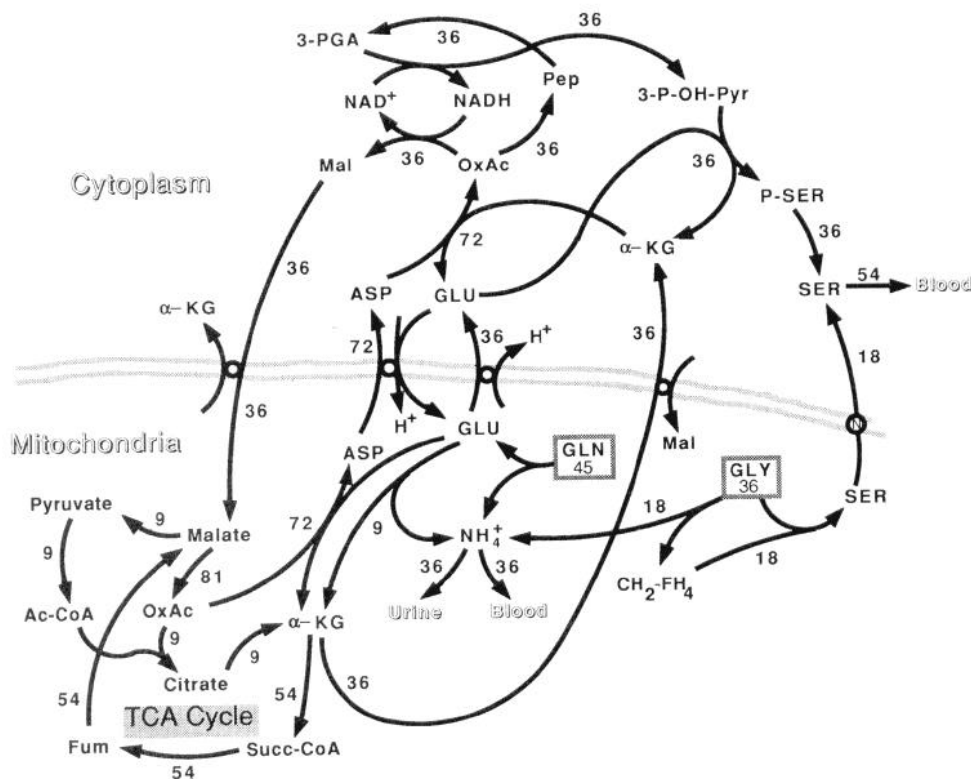
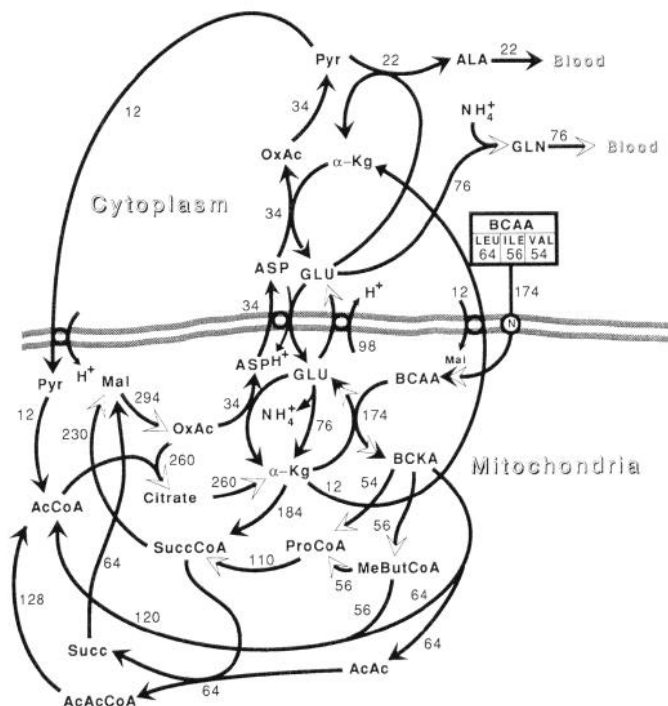


FIG. 10. Details of metabolic process occurring in kidneys during oxidation of daily supply of amino acids in humans. Irregular double line across center represents inner membrane of mitochondria. α -Ketoglutarate-malate antiport has been drawn twice for convenience. Data needed for accurate calculations of metabolic flows in kidney are not available in humans. Ammonium production was partitioned equally between urine and renal vein, although renal vein probably usually receives somewhat $>50\%$. Urinary ammonium was set equal to net metabolic acid load of 36 mmol/day, i.e., dietary arginine plus lysine plus one-half dietary histidine, minus dietary aspartate and glutamate, plus twice dietary cysteine and methionine, minus titratable acidity (set at 16), and minus dietary anions (set at 50). Serine production was set to 54 mmol/day, as required by data of Brosnan (10). Sum of glycine input plus twice glutamine input must equal serine production plus net metabolic acid load. Formation of serine was set at $\frac{2}{3}$ from glutamine and $\frac{1}{3}$ from glycine, but no firm data are available to support this assumption. This requires that glycine input be $\frac{2}{3}$ of serine output and that glutamine input be equal to net metabolic acid load plus $\frac{1}{6}$ of serine output or 45 mmol/day. Note that amount of glutamine oxidized via glutamate dehydrogenase and tricarboxylic (TCA) cycle must equal input amount minus amount converted to serine. With this information all metabolic flows are readily calculated. $\text{CH}_2\text{-FH}_4$, N^5, N^{10} -methylene tetrahydrofolate; 3-P-OH-Pyr, 3-phosphohydroxypyruvate; P-Ser, phosphoserine. For definitions of other abbreviations see Figs. 1 and 6.

FIG. 11. Details of metabolic process occurring in liver during oxidation of daily supply of amino acids in humans. Irregular double line across center represents inner membrane of mitochondria. AcAc, acetoacetate; AcAcCoA, acetoacetyl-CoA; AcCar, acetylcarnitine; α AmAdip, α -aminoadipate; AmOxBut, 2-amino-3-oxobutyrate; Car, carnitine; CH-FH₄, N⁵,N¹⁰-methylenetetrahydrofolate; CH₂-FH₄, N⁵,N¹⁰-methylene-tetrahydrofolate; CysS, cysteine sulfinate; GSAlD, glutamate semialdehyde; GuAc, guanidinoacetate; HCys, homocysteine; α KAdip, α -ketoadipate; α KBut, α -ketobutyrate; α KIC, α -ketoisocaproate; MeMal-CoA, methylmalonyl-CoA; 3-OH-Anthr, 3-hydroxyanthranilate; OH-Pyr, hydroxypyruvate; p-OH Φ Pyr, p-hydroxyphenylpyruvate; ProCoA, propionyl-CoA; Sarc, sarcosine; SulfPyr, sulfinylpyruvate; TCA, tricarboxylic acid cycle. C (open letter) designates a cytoplasmic reaction shown for convenience in matrix. For definitions of other abbreviations see Figs. 1 and 6.

REFERENCES

1. ACHESON, K. J., J. P. FLATT, AND E. JÁQUIER. Glycogen synthesis versus lipogenesis after a 500 gram carbohydrate meal in man. *Metabolism* 31: 1234-1240, 1982.
2. ACHESON, K. J., Y. SCHUTZ, T. BESSARD, K. ANANTHARAMAN, J. P. FLATT, AND E. JÁQUIER. Glycogen storage capacity and de novo lipogenesis during massive carbohydrate overfeeding in man. *Am. J. Clin. Nutr.* 48: 240-247, 1988.
3. ANDERSON, B. S., T. Y. AW, AND D. P. JONES. Mitochondrial transmembrane potential and pH gradient during anoxia. *Am. J. Physiol.* 252 (Cell Physiol. 21): C349-C355, 1987.
4. ATKINSON, D. E., AND E. BOURKE. The role of ureagenesis in pH homeostasis. *Trends Biochem. Sci.* 9: 297-300, 1984.
5. AW, T. Y., AND D. P. JONES. Heterogeneity of pH in the aqueous cytoplasm of renal proximal tubule cells. *FASEB J.* 3: 52-58, 1989.
7. BENDER, D. A. *Amino Acid Metabolism*. New York: Wiley, 1985, p. 34.
8. BERGSTROM, J. D., G. A. WONG, P. A. EDWARDS, AND J. EDMOND. The regulation of acetoacetyl-CoA synthetase activity by modulators of cholesterol synthesis in vivo and the utilization of acetoacetate for cholesterologenesis. *J. Biol. Chem.* 259: 14548-14553, 1984.
9. BIRD, M. I., P. B. NUNN, AND L. A. J. LORD. Formation of glycine and aminoacetone from L-threonine by rat liver mitochondria. *Biochim. Biophys. Acta* 802: 229-236, 1984.
10. BROSNAN, J. T. Studying renal amino acid metabolism in vivo—how and why? *Bull. Can. Biochem. Soc.* 22: 22-27, 1985.
- 10a. BROWN, H. D. *Biochemical Microcalorimetry*. New York: Academic, 1969.
11. CHANG, T. W., AND A. L. GOLDBERG. The origin of alanine produced in skeletal muscle. *J. Biol. Chem.* 253: 3677-3684, 1978.
12. CHEEMA-DHADLI, S., R. L. JUNGAS, AND M. L. HALPERIN. Regulation of urea synthesis by acid-base balance in vivo: role of NH_3 concentration. *Am. J. Physiol.* 252 (Renal Fluid Electrolyte Physiol. 21): F221-F225, 1987.
13. COHEN, N. S., F. S. KYAN, S. S. KYAN, C.-W. CHEUNG, AND L. RAJMAN. The apparent K_m of ammonia for carbamoyl phosphate synthetase (ammonia) in situ. *Biochem. J.* 229: 205-211, 1985.
- 13a. COHEN, S. M. Effects of insulin on perfused liver from streptozotocin-diabetic and untreated rats: ^{13}C NMR assay of pyruvate kinase flux. *Biochemistry* 26: 573-580, 1987.
14. COULSON, R. A., AND T. HERNANDEZ. Source and function of urinary ammonia in the alligator. *Am. J. Physiol.* 197: 873-879, 1959.
15. CUSTOR, J. *Archiv anat. Physiol. Wiss. Med.* 478-504, 1873.
16. DARNELL, J., H. LODISH, AND D. BALTIMORE. *Molecular Cell Biology*. New York: Scientific American Books, 1986, p. 892.
17. DICKENS, F., AND H. WEIL-MAHERBE. 2. Metabolism of normal and tumour tissue. 19. The metabolism of intestinal mucous membrane. *Biochem. J.* 35: 7-15, 1941.
18. EATON, S. B., M. KONNER, AND M. SHOSTAK. Stone agers in the fast lane: chronic degenerative diseases in evolutionary perspective. *Am. J. Med.* 84: 739-749, 1988.
19. ELIA, M., AND G. LIVESEY. Effects of ingested steak and infused leucine on forelimb metabolism in man and the fate of the carbon skeletons and amino groups of branched-chain amino acids. *Clin. Sci. Lond.* 64: 517-526, 1983.
20. FASMAN, G. D. *Practical Handbook of Biochemistry and Molecular Biology*. Boca Raton, FL: CRC, 1989, p. 362.
21. FELDMAN, E. B. *Essentials of Clinical Nutrition*. Philadelphia, PA: Davis, 1988, p. 9.
22. FELIG, P. The glucose-alanine cycle. *Metabolism* 22: 179-207, 1973.
23. FELIG, P., J. WAHREN, AND L. RÅF. Evidence of inter-organ amino-acid transport by blood cells in humans. *Proc. Natl. Acad. Sci. USA* 70: 1775-1779, 1973.
24. FERNLEY, R. T. Non-cytoplasmic carbonic anhydrases. *Trends Biochem. Sci.* 13: 356-359, 1988.
25. FINOCCIARO, G., F. TARONI, AND S. DI DONATO. Glutamate dehydrogenase in olivopontocerebellar atrophies: leukocytes, fibroblasts, and muscle mitochondria. *Neurology* 36: 550-553, 1986.
26. FLATT, J. P. Conversion of carbohydrate to fat in adipose tissue: an energy-yielding and, therefore, self-limiting process. *J. Lipid Res.* 11: 131-143, 1970.
27. FLATT, J. P., AND E. G. BALL. Studies on the metabolism of adipose tissue. XIX. An evaluation of the major pathways of glucose catabolism as influenced by acetate in the presence of insulin. *J. Biol. Chem.* 241: 2862-2869, 1966.
- 27a. FOOD POLICY AND FOOD SCIENCE SERVICE. *Amino Acid Content of Foods and Biological Data on Proteins*. Rome: Food and Agriculture Organization of the United Nations, 1970.
28. HAGENFELDT, L., S. ERIKSSON, AND J. WAHREN. Influence of leucine on arterial concentrations and regional exchange of amino acids in healthy subjects. *Clin. Sci. Lond.* 59: 173-181, 1980.
29. HALPERIN, M. L., M. B. GOLDSTEIN, B. J. STINEBAUGH, AND R. L. JUNGAS. Biochemistry and physiology of ammonium excretion. In: *The Kidney*, edited by D. W. Seldin and G. Giebisch. New York: Raven, 1985, p. 1471-1490.
30. HALPERIN, M. L., AND R. L. JUNGAS. Metabolic production and renal disposal of hydrogen ions. *Kidney Int.* 24: 709-713, 1983.
31. HALPERIN, M. L., P. VINAY, A. GOUGOUX, C. PICHETTE, AND R. L. JUNGAS. Regulation of the maximum rate of renal ammoniogenesis in the acidotic dog. *Am. J. Physiol.* 248 (Renal Fluid Electrolyte Physiol. 17): F607-F615, 1985.
32. HÄUSSINGER, D. Nitrogen metabolism in liver: structural and functional organization and physiological relevance. *Biochem. J.* 267: 281-290, 1990.
33. HUTSON, S. M., T. C. CREE, AND A. E. HARPER. Regulation of leucine and α -ketoisocaproate metabolism in skeletal muscle. *J. Biol. Chem.* 253: 8126-8133, 1978.
34. JUNGGERMANN, K. Metabolic zonation of liver parenchyma. *Semin. Liver Dis.* 8: 329-341, 1988.
35. KANNEL, W., AND T. GORDON. The Framingham diet study: diet and the regulation of serum cholesterol. In: *The Framingham Study: An Epidemiological Investigation of Cardiovascular Disease*. Washington, DC: US Dept. Health, Education & Welfare, National Institutes of Health, 1970, sect. 24.
36. KATZ, J. Determination of gluconeogenesis in vivo with ^{14}C -labeled substrates. *Am. J. Physiol.* 248 (Regulatory Integrative Comp. Physiol. 17): R391-R399, 1985.
37. KEELE, C. A., E. NEIL, AND N. JOELS. *Samson Wright's Applied Physiology*. New York: Oxford Univ. Press, 1982, p. 67.
38. KIKERI, D., A. SUN, M. L. ZEIDEL, AND S. C. HEBERT. Cell membranes impermeable to NH_3 . *Nature Lond.* 339: 478-480, 1989.
39. KLEINER, D. Bacterial ammonium transport. *FEMS Microbiol. Rev.* 32: 87-100, 1985.
40. KLINGENBERG, M. The ADP-ATP carrier in mitochondrial membranes. In: *The Enzymes of Biological Membranes: Membrane Transport*, edited by A. N. Martonosi. New York: Plenum, 1976, vol. 3, p. 383-438.
41. LANOUE, K. F., AND A. C. SCHOOLWERTH. Metabolite transport in mitochondria. *Annu. Rev. Biochem.* 48: 871-922, 1979.
42. LEHNINGER, A. L. *Biochemistry*. New York: Worth, 1975, p. 625.
43. LEMASTERS, J. J. An analysis of ADP-induced oxygen jumps by linear nonequilibrium thermodynamics. *J. Biol. Chem.* 259: 13123-13130, 1984.
44. LETTO, J., M. E. BROSNAN, AND J. T. BROSNAN. Valine metabolism. Gluconeogenesis from 3-hydroxyisobutyrate. *Biochem. J.* 240: 909-912, 1986.
- 44a. LOEWY, A. In: *Oppenheimer's Handbuch der Biochemie*, edited by C. Oppenheimer. Jena: Fischer, 1911, vol. 4, p. 279.
45. LOWRY, M., D. E. HALL, AND J. T. BROSNAN. Serine synthesis in rat kidney: studies with perfused kidney and cortical tubules. *Am. J. Physiol.* 250 (Renal Fluid Electrolyte Physiol. 19): F649-F658, 1986.
46. MALLETT, L. E., J. H. EXTON, AND C. R. PARK. Control of gluconeogenesis from amino acids in the perfused rat liver. *J. Biol. Chem.* 244: 5713-5723, 1969.
47. MCGILVER, R. W. *Biochemistry*. Philadelphia, PA: Saunders, 1983, p. 638.
48. MONTGOMERY, R., R. L. DRYER, T. W. CONWAY, AND A. A. SPECTOR. *Biochemistry*. St. Louis, MO: Mosby, 1977, p. 274.
49. OWEN, E. E., AND R. R. ROBINSON. Amino acid excretion and ammonia metabolism by the human kidney during the prolonged administration of ammonium chloride. *J. Clin. Invest.* 42: 263-276, 1963.

50. PAUL, H. S., AND S. A. ADIBI. Regulation of branched chain amino acid catabolism. In: *Branched Chain Amino and Keto Acids in Health and Disease*, edited by S. A. Adibi, W. Fekl, U. Langenbeck, and P. Schauder. Basel: Karger, 1984, p. 182-219.
51. PILKIS, S. J., C. R. PARK, AND T. H. CLAUS. Hormonal control of hepatic gluconeogenesis. *Vitam. Horm.* 36: 383-460, 1978.
52. POZEFSKY, T., R. G. TANCREDI, R. T. MOXLEY, J. DUPRE, AND J. D. TOBIN. Effects of brief starvation on muscle amino acid metabolism in nonobese man. *J. Clin. Invest.* 57: 444-449, 1976.
53. ROGNSTAD, R. Pyruvate cycling involving possible oxaloacetate decarboxylase activity. *Biochim. Biophys. Acta* 586: 242-249, 1979.
54. SCHOLTE, H. R., AND H. F. BUSCH. Early changes of muscle mitochondria in Duchenne dystrophy. *J. Neurol. Sci.* 45: 217-234, 1980.
55. SCHULZ, A. R. Computer-based method for calculation of the available energy of proteins. *J. Nutr.* 105: 200-207, 1975.
56. SNELL, K. Enzymes of serine metabolism in normal, developing and neoplastic rat tissues. In: *Advances in Enzyme Regulation*, edited by G. Weber. New York: Pergamon, 1984, vol. 22, p. 325-400.
57. SQUIRES, E. J., D. E. HALL, AND J. T. BROSNAN. Arteriovenous differences for amino acids and lactate across kidneys of normal and acidotic rats. *Biochem. J.* 160: 125-128, 1976.
58. STERN, J. A role of acetoacetyl-CoA synthetase in acetoacetate utilization by rat liver cell fractions. *Biochem. Biophys. Res. Commun.* 44: 1001-1007, 1971.
59. STILES, P. G., AND G. LUSK. On the action of phlorhizin. *Am. J. Physiol.* 10: 67-79, 1903.
60. STRZELECKI, T., K. F. LANOUE, AND J. A. THOMAS. Hormonal effects on intracellular proton compartmentation in hepatocytes. In: *Isolation, Characterization and Use of Hepatocytes*, edited by R. A. Harris and N. W. Cornell. New York: Elsevier Biomedical, 1983, p. 303-310.
61. TIZIANELLO, A., G. DEFERRARI, G. GARIBOTTO, C. ROBAUDO, N. ACQUARONE, AND G. M. GHIGGERI. Renal ammoniogenesis in an early stage of metabolic acidosis in man. *J. Clin. Invest.* 69: 240-250, 1982.
62. VINAY, P., A. GOUGOUX, AND G. LEMIEUX. Isolation of a pure suspension of rat proximal tubules. *Am. J. Physiol.* 241 (Renal Fluid Electrolyte Physiol. 10): F403-F411, 1981.
63. VORHABEN, J. E., AND J. W. CAMPBELL. Glutamine synthetase. A mitochondrial enzyme in uricotelic species. *J. Biol. Chem.* 247: 2763-2767, 1972.
64. WAGENMAKERS, A. J. M., H. J. M. SALDEN, AND J. H. VEERKAMP. The metabolic fate of branched-chain amino acids and 2-oxo acids in rat muscle homogenates and diaphragms. *Int. J. Biochem.* 17: 957-965, 1985.
65. WILSON, T. H., AND G. WISEMAN. Metabolic activity of the small intestine of the rat and golden hamster (*Mesocricetus auratus*). *J. Physiol. Lond.* 123: 126-130, 1954.
66. WINDMUELLER, H. G., AND A. E. SPAETH. Intestinal metabolism of glutamine and glutamate from the lumen as compared to glutamine from blood. *Arch. Biochem. Biophys.* 171: 662-672, 1975.
67. WINDMUELLER, H. G., AND A. E. SPAETH. Metabolism of absorbed aspartate, asparagine, and arginine by rat small intestine in vivo. *Arch. Biochem. Biophys.* 175: 670-676, 1976.
68. WINDMUELLER, H. G., AND A. E. SPAETH. Respiratory fuels and nitrogen metabolism in vivo in small intestine of fed rats. *J. Biol. Chem.* 255: 107-112, 1980.
69. WINDMUELLER, H. G., AND A. E. SPAETH. Source and fate of circulating citrulline. *Am. J. Physiol.* 241 (Endocrinol. Metab. 4): E473-E480, 1981.
70. ZUBAY, G. *Biochemistry*. Reading, MA: Addison-Wesley, 1983, p. 449.